This is a preprint, the final version is subject to change, of the American Mineralogist (MSA)
Cite as Authors (Year) Title. American Mineralogist, in press.
DOI: https://doi.org/10.2138/am-2019-6751

Revision 2

Carbon and nitrogen isotopes and mineral inclusions in diamonds from chromitites of the Mirdita ophiolite (Albania) demonstrate recycling of oceanic crust into the mantle

Weiwei Wu[1*,2], Jingsui Yang[2], Richard Wirth[3], Jianping Zheng[1], Dongyang Lian[2], Tian Qiu[2], Ibrahim Milushi[4]

1. College of Marine Science and Technology, China University of Geosciences (Wuhan), No. 388 Lumo Road, Wuhan 430074, China
2. Key Laboratory of Deep-Earth Dynamics of MLR, Institute of Geology, Chinese Academy of Geological Sciences, No. 26 Baiwanzhuang Road, Beijing 100037, China
3. Helmholtz Centre Potsdam, GFZ German Research Center for Geosciences, Telegrafenberg, Section 4.4, D-14473 Potsdam, Germany
4. Institute of Geosciences, Energy, Water and Environment, Polytechnic University of Tirana, Rruga: Don Bosko nr. 60, Tirana 1000, Albania

Corresponding author: Weiwei Wu, E-mail: cugcags@163.com;

Co-authors:

Yang's E-mail: yangjsui@163.com;

Wirth's E-mail: wirth@gfz-potsdam.de;

Zheng's E-mail: jpzheng@cug.edu.cn;

Lian's E-mail: ldy199008@163.com;

Qiu's E-mail: qiutian2010@126.com;

Milushi's E-mail: ibrahimmilushi@yahoo.com

Always consult and cite the final, published document. See http:/www.minsocam.org or GeoscienceWorld

ABSTRACT

Geophysical investigations and laboratory experiments provide strong evidence for subduction of ancient oceanic crust, and geological and mineralogical observations suggest that subducted oceanic crust is recycled into the upper mantle. This model is supported by some direct petrologic and mineralogical evidence, principally the recovery of super-deep diamonds from kimberlites and the presence of crustal materials in ophiolitic chromitites and peridotites, but many details are still unclear. Here we report the discovery of ophiolite-hosted diamonds in the podiform chromitites of the Skenderbeu massif of the Mirdita ophiolite in the western part of Neo-Tethys. The diamonds are characterized by exceedingly light C isotopes ($\delta^{13}C_{PDB} \sim -25‰$), which we interpret as evidence for subduction of organic carbon from Earth's surface. They are also characterized by an exceptionally large range in $\delta^{15}N_{air}$ (-12.9‰ to +25.5‰), accompanied by a low N aggregation state. Materials sparsely included in diamonds include amorphous material, Ni-Mn-Co alloy, nanocrystals (20 x 20 nm) of calcium silicate with an orthorhombic perovskite structure (Ca-Pv), and fluids. The fluids coexisting with the alloy and Ca-Pv provide clear evidence that the diamonds are natural rather than synthetic. We suggest that the Skenderbeu diamonds nucleated and grew from a C-saturated, NiMnCo-rich melt derived from a subducted slab of ocean crust and lithosphere in the deep mantle, at least in the diamond stability field, perhaps near the top of the mantle transition zone. The subsequent rapid upward transport in channelled networks related to slab rollback during subduction initiation may explain the formation and preservation of Skenderbeu diamonds. The discovery of diamonds from the Mirdita ophiolite not only provides new evidence of diamonds in these settings, but also provides a valuable opportunity to understand deep cycling of subducted oceanic crust and mantle composition.

Always consult and cite the final, published document. See http:/www.minsocam.org or GeoscienceWorld

Key words: Mirdita ophiolite, Diamond, NiMnCo alloy, Calcium silicate perovskite, Carbon and nitrogen isotopes, Subduction, West Albania

INTRODUCTION

It has become apparent over the last decade that there are a variety of diamond-forming processes in the mantle that can be linked to major geologic events. For many years it was assumed that diamonds occur in only three geological setting: (1) in cratonic mantle (carried to Earth's surface by kimberlite, lamproite, and lamprophyre); (2) in ultra-high pressure (UHP) metamorphic rocks such as gneiss and eclogite exhumed by slab rollback in continent-continent collision zones; and (3) in meteorite impact craters (Sobolev and Shatsky 1990; Xu et al. 1992; Koeberl et al. 1995; Goresy et al. 2001; Shirey et al. 2013). Studies of mineral inclusions in kimberlite diamonds (e.g., Stachel and Harris 2008; Shirey et al. 2013; Stachel and Luth 2015) have shown that such diamonds are derived mostly from the subcontinental lithospheric mantle at depths below about 150-200 km along both continental and oceanic geothermal gradients, and from convecting mantle beneath the lithosphere-asthenosphere boundary (Stachel et al. 2005). Some diamonds may have originated at even greater depths (>700 km) in the sublithospheric mantle/asthenosphere mantle. However, the actual abundance of diamonds formed below the lithosphere is not known and may be much larger than what has been erupted in kimberlites and other diamond-hosting rocks (Shirey et al. 2013). Thus, the estimated volume of diamonds in Earth may reflect the availability of transport mechanisms that can bring diamonds to the surface without their being graphitized or oxidized.

In recent years a number of other diamond-hosting rocks have been identified including: (1) volcanic rocks, such as picrites (Golovko and Kaminsky 2010), meimechites (Kaminsky 2007; Kaminsky et al. 2016), and basalt (Kaminsky et al. 2016); (2) plutonic rocks, such as peridotites and chromitites (Pearson et al. 1989; Bai et al. 1993) and pyroxenites (Kaminsky 2007).

Always consult and cite the final, published document. See http:/www.minsocam.org or GeoscienceWorld

Diamonds were first reported in ophiolitic chromitites and peridotites by Bai et al. (1993) but these discoveries were largely ignored or simply attributed to natural or anthropogenic contamination. Since that time numerous ultrahigh-pressure and highly reduced phases, accompanied by a wide range of other exotic minerals, have been reported from peridotites and chromitites in several Tibetan ophiolites and eleven other ophiolite massifs in six suture zones by researchers at the Chinese Academy of Geological Sciences (Robinson et al. 2004; Yang et al. 2007, 2014, 2015a, 2015b; Huang et al. 2015; Lian et al. 2017; Xiong et al. 2017; Wu et al. 2017), as well as other independent research groups (Dobrzhinetskaya et al. 2009; Yamamoto et al. 2009; Arai 2013; Galuskin et al. 2013; Howell et al. 2015; McGowan et al. 2015; Griffin et al. 2016). Concerns about the significance of these findings were eventually overcome by the discovery of in-situ grains (e.g. Yang et al. 2007, 2014, 2015a; Das et al. 2015, 2017; Liang et al. 2014; Zhang et al. 2016). Confirmation that diamonds and other exotic minerals are widespread in ophiolite massifs challenges existing models of Earth processes and requires a new paradigm to explain how and where they formed in the mantle (Yang et al. 2007; Arai 2013; Zhou et al. 2014; Howell et al. 2015; Griffin et al. 2016; Lian et al. 2017).

Most of the original discoveries of diamonds were in Neo–Tethys ophiolites of southern Tibet in the eastern part of the belt, thus raising the question of whether they were present in other parts of the system. Lian et al. (2017, 2018) reported diamonds from podiform chromitites in the Pozanti-Karsanti ophiolites, Turkey. Here we present new data on the exotic minerals in the Skenderbeu massif located in the Mirdita ophiolite (Wu et al. 2017), which occur in the western part of Neo–Tethys, and discuss their tectonic significance.

Here we provide direct evidence that the Skenderbeu diamonds are indigenous rather than contaminants, present a new model for the origin of the alloys within the diamonds, and discuss these exotic minerals with special reference to the role of plate subduction.

Always consult and cite the final, published document. See http:/www.minsocam.org or GeoscienceWorld

GEOLOGICAL SETTING

The Mesozoic ophiolites in the eastern Mediterranean region occur along nearly E-W-trending, curvilinear suture zones (Fig. 1a) separating a series of Gondwana-derived continental blocks. The ophiolites represent the remnants of Tethyan oceanic lithosphere that developed in different seaways, between these microcontinents (Shallo et al. 1990; Dilek 2003; Saccani and Photiades 2004; Saccani and Tassinari 2015). The Jurassic ophiolites in the Albanide-Hellenide segment of the Alpine orogenic system are relics of the Mesozoic Pindos-Mirdita marginal basin, which developed between the Apulia and Pelagonia-Korabi microcontinents. These ophiolites are underlain by discontinuously exposed meta-mafic and meta-pelitic rocks and mélanges, which include blocks and clasts of ophiolitic and rift-drift-related volcanic–sedimentary rock units in a sedimentary matrix (Shallo et al. 1990; Shallo and Dilek 2003; Dilek et al. 2005). The ophiolites are unconformably overlain by supra-ophiolitic mélanges and Middle Cretaceous and younger, undeformed, neritic carbonates, indicating that ophiolite emplacement in the region was completed by the early Cretaceous (Chiari et al. 2004; Shallo and Dilek 2003).

Early studies in the Mirdita ophiolite zone led to the recognition of two types of ophiolites with distinct geology, petrology, geochemistry, and tectonic setting of formation (Shallo et al. 1990; Beccaluva et al. 1994; Hoeck et al. 2002). The western Mirdita ophiolite has been interpreted as a relic of Jurassic oceanic lithosphere developed at a mid-oceanic ridge environment (MOR ophiolite), whereas the eastern Mirdita ophiolite is thought to be a remnant of a suprasubduction zone (SSZ) mantle wedge generated within the same basin. These models, hence, envision two discrete tectonic settings of formation for the western and eastern Mirdita ophiolite separated in time and space. However, other studies have shown that this two-fold subdivision is not as sharp as previously thought (e.g., Hoeck et al. 2002; Dilek and Flower 2003; Koller et al. 2006; Dilek and Morishita 2009; Wu et al. 2018).

Always consult and cite the final, published document. See http:/www.minsocam.org or GeoscienceWorld

The Mirdita ophiolite zone in the northern Albanides is nearly 30 km wide in a NW-SE direction and is bounded by conjugate passive margin sequences of Apulia on the west and Korabi–Pelagonia on the east (Fig. 1b). Magnetic and gravity anomalies show a >15-km-thick, mafic-ultramafic slab with a large synform structure between these continental blocks (Frasheri et al. 1996). Large peridotite massifs associated with ophiolitic crustal units occur on both sides of this synform structure and adjacent to the continental blocks. Adjacent to the Apulian continental margin on the west, these peridotite massifs (Krrabi, Puke, Gomsiqe, Skenderbeu) consist mainly of plagioclase lherzolites, whereas those close to Pelagonia to the east (Kukesi, Lure, Bulquiza, Shebenique) are composed of depleted harzburgites, dunites and podiform chromitites (Fig. 1b; Shallo et al. 1990; Hoxha and Boullier 1995; Shallo and Dilek 2003; Dilek et al. 2005; Shenjatari and Beqiraj 2010).

The Skenderbeu massif occurs in the western Mirdita ophiolite in the northern Albanides and is unconformably (but locally tectonically) overlain by Cenozoic terrestrial sedimentary deposits of the NW–SE–oriented Burrell basin (Fig. 1b). It is juxtaposed on the west against Triassic–Jurassic carbonate rocks of the pre-Apulian platform along WNW – vergent thrust and transpressional fault systems (Dilek et al. 2005). The massif includes, from west to east, harzburgites with dunite lenses and minor chromitites, lherzolites, and layered dunites–troctolites and gabbros at the top (Fig. 2). Basaltic pillow lavas rest directly on the peridotites and ultramafic cumulates along E – dipping normal faults (Fig. 2). These pillow lavas are unconformably overlain by a chaotic volcanic – sedimentary unit, locally olistostromal in nature, that displays gentle to open folds. This unit is thought to be a latest Jurassic–Cretaceous supra–ophiolitic mélange (Fig. 2; Shallo and Dilek 2003), which likely developed during the early stages of basin-wide contraction and closure (Dilek et al. 2005).

SAMPLES AND ANALYTICAL PROCEDURES

Always consult and cite the final, published document. See http:/www.minsocam.org or GeoscienceWorld

We collected nearly 600 kg of massive chromitite from the Skenderbeu massif (Fig. 2, Wu et al. 2017). Initial mineral separation was carried out at the Institute of Multipurpose Utilization of Mineral Resources, Chinese Academy of Geological Sciences, Zhengzhou. The detailed mineral separation procedure has been described by Xu et al. (2009). In order to avoid any contamination, we selected only unaltered samples of massive chromitite that were free from veins or dikelets.

Thus far we have identified more than 20 grains of diamond from the Skenderbeu chromitite (Fig. 3, Wu et al. 2017). They are mostly light yellow, transparent, euhedral crystals, 100-200 μm across, with a range of morphologies (Fig. 3); some are octahedral and cuboctahedral and others are elongate and irregular (Fig. 3a, 3b). All of the diamond grains have yielded typical Raman spectra with a peak at ~1325 cm^{-1} (Fig. 3d). These diamonds are similar in morphology to grains recovered from other ophiolites but are generally a little smaller and less abundant. See Supplementary Data for full analytical details.

RESULTS

Carbon isotopic composition

The carbon isotopic compositions of twelve diamonds were measured by SIMS on one or two points within each grain yielding a total of 18 analyses. The average and the range of carbon isotopic composition observed in each diamond is reported in Table 1. Isotopic compositions range from −27.6 to −23.8‰ (rel. to PDB) (Fig. 4), with an average of −25.8‰, similar to the ranges observed from surface organic material, which has a mean $\delta^{13}C$ of approximately −25 ‰ (Cartigny 2005). All of the Skenderbeu diamonds are $\delta^{13}C$-depleted when compared with mantle carbon values (−5 ‰). Two of the analysed diamonds show slightly variable $\delta^{13}C$ compositions, with differences of 0.7 ‰ between measurements within a single sample (Table 1, Fig. 4).

Always consult and cite the final, published document. See http:/www.minsocam.org or GeoscienceWorld

Cathodoluminescence (CL) images of twelve diamond samples from the epoxy mounts are shown in Fig. 4. They all reveal clear sector growth zoning (Howell et al. 2015). Measured $\delta^{13}C$ varies no more than ~ 0.7 ‰ between sectors (sample E180-4, –25.7 to –26.4 ‰).

Nitrogen abundance and isotopic composition

SIMS analyses of 8 Skenderbeu diamonds yield N concentrations ranging from 37 to 286 ppm with a median of 135 ppm (Table 1, Fig. 4). These diamonds exhibit a wide range in $\delta^{15}N_{AIR}$ from –12.9‰ to +25.5‰ with a median of +1.9‰ (Table 1, Fig. 4). There are noticeable nitrogen concentration differences between octahedral and cubic growth sectors (Fig. 5); the data do not permit evaluation of intersectoral concentration variability. In general, the $\delta^{15}N_{AIR}$ values of the octahedral sectors are either similar to, or slightly higher than, those of the cubic sectors (Fig. 5), similar to results for other occurrences reported by Howell et al. (2015). Overall, there is no statistically significant relationship between $\delta^{13}C_{PDB}$ and $\delta^{15}N_{AIR}$ in the Skenderbeu diamonds. The stable isotope values are akin to carbonado (Fig. 5; Haggerty 2017).

Mineral inclusions

A total of three mineral inclusions were found in two TEM foils: inclusions 1 and 2 in foil E180-1#5006 and inclusion 3 in foil E180-5#5010 (Figs. 6 - 10). In addition to the inclusions, the diamonds show many crystal defects such as dislocations (Fig. 6, 8). Two types of dislocations are present: (a) curved dislocation lines that are indicative of dislocation climb, high-temperature deformation and early stage recovery and (b) long, straight dislocations that are indicative of dislocation glide during high-temperature deformation without recovery (Hull and Bacon 2011).

Monophase inclusions. Inclusions 1 and 2 range in size from 1000 to 1500 nm in their longest dimension and are single-phase materials (Fig. 6a, 6b, 6c). The matrix consists mainly of

Always consult and cite the final, published document. See http:/www.minsocam.org or GeoscienceWorld

carbon, silicon, oxygen, magnesium, with minor sulfur and chlorine, and low aluminium and iron (Fig. 7). The weak X-ray intensities of Cu–Kα and Ga–Kα as well as Cu–L, Ga–L in the spectra are due to the copper grid and some Ga implanted during foil preparation. The absence of lattice fringes and thus of a diffraction pattern (fast Fourier Transform, FFT) using high-resolution electron microscopy (HREM) prove that inclusions 1 and 2 are amorphous. In electron energy-loss spectra (EELS) of inclusions 1 and 2, the oxygen K-edge at approximately 532 eV of inclusion 2 (peak a in Fig. A1a) indicates the presence of oxygen (Kurata et al. 1993). The onset of the carbon K-edge at approximately 286 eV (peak π* in Fig. A1b, Fig. A1c) and at approximately 294 eV (peak σ* in Fig. A1b, Fig. A1c) reveal the difference with diamond (Egerton and Whelan 1974), because the carbon K-edge onset from diamond has shifted to higher energy loss (Egerton and Whelan 1974; Garvie et al. 1995). The inclusions also produce a broad, featureless σ* peak, indicating sp^2 bonding configurations, which are typical of amorphous carbon (Katrinak et al. 1992).

Multiphase inclusion. Inclusion 3 is an oval (approximately 104 × 60 nm), multiphase inclusion (Fig. 8). The high-angle annular dark field (HAADF) image (Z-contrast imaging) in Fig. 8b shows a bright Ni-Mn-Co alloy with weakly developed crystal faces, together with some dark grey pores filled with a fluid phase and a light grey, nanocrystalline silicate phase. The alloy phase is composed of Ni, Mn and Co (at %) ~ 68.3; 27.3; 4.4, respectively (Fig. 9b). The blue rectangles in Fig. 8b indicate the area of the phase that was analysed. The Si Kα and Cl Kα X-ray intensities displayed in the spectrum are due to the presence of silicate material and/or the fluid phase above or below the alloy.

The silicate phase was identified as a Ca-silicate perovskite nanocrystal (approx. 20 x 20 nm). An energy dispersive X-ray analysis (EDX) spectrum (Fig. 9a) shows that it is dominated by Si- Ca-Mn and O. The crystal structure was identified based on electron diffraction data

Always consult and cite the final, published document. See http:/www.minsocam.org or GeoscienceWorld

derived from HREM images and the calculated diffraction pattern (Fig. 10a,b), and a comparison of the observed d-spacings and the angles between adjacent planes with those of calculated data for Ca-silicate perovskites with orthorhombic and tetragonal structures. The observed d-spacings and angles match closely the data for an orthorhombic structure (Table 2). Based on the chemical composition and crystalline structure, the silicate inclusions associated with the metallic alloys are determined to be $(Ca_{0.81}Mn_{0.19})(SiO_3)$ (Fig. 8b), hereafter termed Mn-bearing Ca-Pv. The analysed area in Fig. 8b includes some pores that might still be filled with fluid (discussed below), which may account for the Cl and K peaks in the spectrum (Fig. 9a).

The Mn-bearing Ca-Pv is associated with small, fluid-filled pores at the interface of the inclusion and the host diamond (indicated by blue arrows in Fig. 8b). Although the fluids may have been lost during preparation of the FIB foils, two EDX spectra of material on the walls of the pores (Fig. 9c, d) show the presence Cl and K, with or without Mg**.** The other elements in the spectra (Ni, Mn, Co, Si and Ca) are from the other phases in this inclusion. The presence of a fluid associated with the silicate phase and metal alloy completely exclude any possibility that this diamond is synthetic. Synthetic diamonds precipitated from a metal alloy would never contain fluid inclusions.

DISCUSSION

Natural origin of the Skenderbeu diamonds

Podiform chromitites have long been thought to form through reaction between mantle peridotite (especially harzburgite) and melt, with subsequent magma/melt mixing at an uppermost mantle level (<30 km, Arai and Yurimoto 1994; Zhou et al. 1994; Arai 1997, 2013). However, the ultra-high pressure (UHP)-super reduced (SuR) minerals that have been recovered from numerous ophiolites over the last 15 years (Robinson et al. 2004; Yang et al. 2007, 2014,

Always consult and cite the final, published document. See http:/www.minsocam.org or GeoscienceWorld

2015a, 2015b; Yamamoto et al. 2009; Xu et al. 2009; Lian et al. 2017; Wu et al. 2017), require some rethinking of this model. Recently, a lightning-strike formation mechanism has been proposed for the origin of UHP and SuR minerals in ophiolites (Ballhaus et al. 2017, 2018). We conclude, however, that such a process can hardly be an important source of UHP and SuR minerals in ophiolites based on (1) the common occurrence of these UHP and SuR minerals in different ophiolites (Yang et al. 2015a; Zhang et al. 2016; Das et al. 2017; Wu et al. 2017); (2) the occurrence of in situ diamond associated with amorphous carbon (Yang et al. 2015a) and in situ SuR phases (Zhang et al. 2016); (3) the isotopic compositions and trace element concentrations of these diamonds (Howell et al. 2015a; Yang et al. 2015a); (4) the mineral inclusions such as IR-active water, solid CO_2, and carbonate and silicate fluid inclusions are exclusive to natural diamonds (Moe et al. 2018; Yang et al. 2018), and the results of our own research. However, the formation process for ophiolite-hosted diamonds is still poor understood.

Although a wide variety of SuR-UHP minerals have been recovered from ophiolites, the discovery of widespread diamond aroused the most controversy (Griffin et al. 2016). The diamonds from Luobusa have been reported and described in several papers (Robinson et al. 2004; Yang et al. 2007, 2014; Xu et al. 2009, 2015) and characterized in detail by Howell et al. (2015) and Moe et al. (2018). Howell et al. (2015) pointed out that Luobusa diamonds show many similarities with those synthesized by HP/HT industrial methods, but there are also important differences in their morphology, inclusions and trace element concentrations. Recently, the Gemological Institute of America (GIA) confirmed that the diamonds discovered in Luobusa and Ray-Iz ophiolites originated from a geological environment very different from that in which natural gem-quality diamonds are formed (Moe et al. 2018). The presence of fluid inclusions in these diamonds clearly distinguish them from diamond synthesized from pure metal or alloy solvent which is a completely dry system. Typically, such synthetic diamonds contain

Always consult and cite the final, published document. See http:/www.minsocam.org or GeoscienceWorld

only solid inclusions with the chemical composition of the host alloy (Smith and Wang 2016; Moe et al. 2018). At this point, we can say that anthropogenic contamination can be ruled out and that these discoveries point to previously unrecognized compositional heterogeneity of the oceanic mantle and provide evidence of extensive recycling of crust-mantle material.

Inclusions in the Skenderbeu diamonds: Evidence for origin from Earth's mantle

On the basis of morphology and internal growth structures, natural diamonds are normally believed to crystallize in the mantle from fluids/melts (varying from C-O-H-rich to carbonatitic and silicate-rich) rather than from alloy melts (Harte 2010). Because diamond stability requires formation at pressures in excess of 4.5 to 5 GPa (~150 km depth), fluids of these compositions will show considerable miscibility with one another (Litvin et al. 2008; Harte 2010). The precipitation of diamond from fluids/melts is commonly believed to be caused by reduction/oxidation events (Taylor and Green 1989), and this has also been proposed for "superdeep" diamonds (Stachel 2001; Bulanova et al. 2010; Harte 2010). During growth, diamonds commonly incorporate small volumes of fluid/melt, as well as crystalline phases. Once trapped inside a diamond, the inclusions are protected from the surrounding media, and are therefore believed to maintain constant chemical compositions. Thus, geochemical studies on mineral inclusions in diamonds have fundamentally changed and shaped our understanding of where, when and how ophiolite-hosted diamonds form, as well as of the chemical and physical nature of mantle environments in which other natural diamonds grow (Shirey et al. 2013; Stachel and Harris 2008; Smith et al. 2015; Stachel and Luth 2015; Jablon and Navon 2016).

Stachel and Harris (2008) presented a comprehensive review of inclusions in diamonds formed in the lithospheric mantle. Silicate inclusions in such diamonds are commonly classified into 2 dominant parageneses; peridotitic (P-type, with harzburgitic and lherzolitic members) and eclogitic (E-type). A minor websteritic paragenesis is present at some localities and a wehrlitic

Always consult and cite the final, published document. See http:/www.minsocam.org or GeoscienceWorld

paragenesis has also been tentatively identified (Stachel and Harris 2008; Shirey et al. 2013). P-type diamonds mainly include typical mantle minerals, such as Cr-pyrope, Mg-olivine, Cr-clinopyroxene, orthopyroxene and chromite, whereas E-type diamond commonly contain inclusions of omphacite, FeAl-garnet, phlogopite, coesite and rutile (Sobolev et al. 1997; Yang et al. 2015a).

The study of mineral inclusions in sublithospheric diamonds is in a youthful stage compared to the study of inclusions in lithospheric diamonds due to the rarity of specimens, small grain sizes, and difficulties in distinguishing original high-pressure minerals from their low-pressure, retrograde assemblages (Shirey et al. 2013). Such retrograde assemblages may closely match silicate mineral assemblages determined by high pressure and temperature experimental studies for the depths in the Earth's mantle (Kaminsky 2017). Notwithstanding, sublithospheric diamonds can also be divided into ultramafic (peridotitic) and basaltic (eclogitic) types on the basis of their inclusions (Stachel and Harris 2008; Harte 2010; Shirey et al. 2013). Ultramafic inclusions are characterized by high-pressure magnesium-rich phases such as Mg-perovskite, ringwoodite, wadsleyite, and olivine with ferro-periclase, majorite, and Ca-perovskite and their low-pressure breakdown products. Basaltic inclusions show associations involving majorite, clinopyroxene, CaTi-perovskite, Ca-perovskite, Ca-ferrite, stishovite, and the "new aluminum phase" (NAL; Shirey et al. 2013; Kaminsky 2017). Inclusion compositions in diamonds formed in the subcratonic mantle are buffered by the compositions of the local lithologies, as well as the distribution of hydrous minerals and the loci where dehydration reactions take place in subducting slabs to release H_2O, which may then cause melting.

Detailed descriptions of inclusions in diamonds from UHP (ultrahigh-pressure metamorphic) terranes (Dobrzhinetskaya et al. 2001, 2003a, 2003b; Dobrzhinetskaya 2012) have shown that these are very different from those in ophiolite-hosted diamonds. Solid inclusions in diamond of

Always consult and cite the final, published document. See http:/www.minsocam.org or GeoscienceWorld

the Kokchetav massif, Kazakhstan are represented by oxide suites of SiO_2, TiO_2, Fe_XO_Y, Cr_2O_3, Th_XO_Y, and rare inclusions of $ZrSiO_4$, $BaSO_4$, $MgCO_3$, $CaCO_3$-aragonite, and a single inclusion of a stoichiometric Fe-rich pyroxene. A suite of oxide nanoinclusions such as SiO_2, TiO_2, Al_2O_3, Pb_XO_Y and Al_2SiO_5 has also been found in diamonds from the Erzgebirge massif, Germany (Dobrzhinetskaya et al. 2003b, 2010; Dobrzhinetskaya 2012).

Fluid inclusions in diamonds from both of these massifs are characterized by "carbonate-water" (e.g., oxidized species), suggesting a relatively high oxidation state of the diamond-forming fluid (Dobrzhinetskaya 2012). The abundance of inclusions from the above occurrences support strongly the hypothesis that diamonds from UHP terranes are crystallized from carbon dissolved in C-O-H supercritical fluids/melts circulating between subducting slabs and the overlying mantle wedge (Dobrzhinetskaya 2012).

The character and compositions of inclusions in ophiolite-hosted diamonds have been documented in numerous papers during the past decade (Yang et al. 2015b; Dobrzhinetskaya et al. 2009; Howell et al. 2015; Griffin et al. 2016). The most common inclusions are NiMnCo alloys, and manganese-rich minerals such as spessartine, tephroite, MnO (Yang et al. 2015b), and coesite. When such inclusions were first reported in ophiolite-hosted diamonds they were thought to be a unique assemblage, found in no other diamonds. However, very similar inclusions have now been reported in Precambrian diamonds from Dachine, French Guiana (Smith et al. 2016a). Interestingly the Dachine diamonds have other features similar to those of the ophiolite-hosted varieties, including light C isotopes and low aggregation states of N. Like the ophiolite-hosted diamonds they are thought to reflect subduction of oceanic crust and surface organic material into the mantle (Smith et al. 2016a).

On the basis of their morphology and composition, we suggest that the inclusions in the Skenderbeu diamonds (Figs. 6 and 8) are syngenetic with their host (Table 2). The presence of

Always consult and cite the final, published document. See http:/www.minsocam.org or GeoscienceWorld

amorphous carbon in inclusions 1 and 2 (Fig. A1) suggests the original presence of a high-density, carbon-rich fluid that was the source of carbon which may have been dissolved in a carbon- oversaturated NiMnCo alloy melt.

Although very little work has been done on the Ni-Mn-Co ternary system, a few investigations indicate a minimum melting temperature of ~1227°C at 1 atm (Gokcen 1991; Gupta 1999), which would correspond to a pressure of 5-6 GPa, equivalent to a depth of 150 – 200 km. The liquidus and solidus of the Mn-Ni system (Co can be neglected because the concentration is low) at high pressure can be calculated from thermodynamic data (Guo and Du 2005 and references therein), and they show that the melting temperature is obviously higher under mantle conditions. For instance, at 3 GPa the melting temperature can be ~1328°C (Guo and Du 2005), which means that the onset of NiMnCo alloy melting should be deeper than 150 – 200 km.

Measurements of garnet peridotites from cratonic lithosphere show that fO_2 generally decreases with depth; at approximately 8 GPa (~250 km), mantle fO_2 will be 5 log units below the fayalite-magnetite-quartz oxygen buffer, and Fe-Ni alloy can be formed as a result of the abundance of FeO (Frost and McCammon 2008). It is possible that at this level (>250 km) the mantle will be metal saturated. Similar metallic melts have been suggested to account for the growth of natural diamonds at depths greater than ~250 km (Jacob et al. 2004; Kaminsky and Wirth 2011; Smith et al. 2016b), where metal becomes stable. We suggest that the NiMnCo alloy inclusions reported here are samples of this alloy melt saturated at depth below 250 km. The metallic inclusions may be direct evidence of charge disproportionation and the resulting limited activity of oxygen in the deep upper mantle. The high concentration of nickel in the NiMnCo alloys in the Skenderbeu diamonds probably originated from an Fe-Ni alloy. It is still not clear why there is no Fe in these alloys but it could have been removed as native iron, Fe-carbides or

Always consult and cite the final, published document. See http:/www.minsocam.org or GeoscienceWorld

other highly-reduced phases observed in the Luobusa mineral separates (Yang et al. 2014, 2015a, 2015b; Howell et al. 2015).

Perovskite ($CaSiO_3$) is chemically unusual because it rarely forms solid solutions with other cations, especially divalent cations (Fujino et al. 2008; Li et al. 2015). However, the Goldschmidt tolerance factor (a dimensionless number calculated from the ratios of the ionic radii that is an indicator for the stability and distortion of perovskite structures, Leinenweber et al. 1991) is 0.93 for $MnSiO_3$ perovskite, which is comparable to that of $CaSiO_3$ perovskite (0.99). This suggests that Ca-Pv can have small amounts of Mn (Fujino et al. 2008; Li et al. 2015), similar to the inclusions in the Skenderbeu diamonds (($Ca_{0.81}Mn_{0.19}$) (SiO_3)). The observed d-spacings and angles of the Mn-bearing Ca-Pv inclusion of the Skenderbeu diamond are consistent with an orthorhombic structure (Table 2, Fig. 10). By using density functional simulations, within the generalized gradient approximation and the projector augmented wave method, Jung and Oganov (2005) demonstrated that the $CaSiO_3$ perovskite phase transforms to a tetragonal structure at 14.2 GPa (~430 km), which suggests the Skenderbeu diamonds originated no deeper than the uppermost part of the mantle transition zone (MTZ). This conclusion is also supported by high-pressure experiments (Zhang et al. 2017; Akaogi et al. 2018).

Subducted source of isotopically light carbon

Carbon and nitrogen isotopic compositions of diamonds are the most common tools used to determine the source of diamond-forming material and to model the processes involved in diamond formation (Cartigny et al. 1998; Thomassot et al. 2007; Palot et al. 2012; Mikhail et al. 2013). It is widely believed that the mantle has a relatively uniform carbon isotopic composition of $\delta^{13}C \sim -5‰$, a composition reflected in the worldwide kimberlite diamond population (Cartigny 2005). All of the Skenderbeu diamonds are obviously $\delta^{13}C$-depleted compared to the

Always consult and cite the final, published document. See http:/www.minsocam.org or GeoscienceWorld

assumed mantle value and have relatively uniform carbon isotopic compositions, ranging from −27.6 to −23.8 (PDB) (average = −25.8‰) (Fig. 4) All analysed ophiolite-hosted diamonds have similar isotopically light compositions and such values have even been reported in some cratonic mantle diamonds (Bulanova et al. 2010; Smart et al. 2011; Walter et al. 2011; Schulze et al. 2013; Thomson et al. 2014). There are three main hypotheses for the origin of isotopically light carbon: (1) a distinct primordial reservoir in the mantle (Palot et al. 2012); (2) fractionation of the main carbon reservoir in the mantle (Cartigny et al. 1998; Stachel 2001; Thomassot et al. 2007); and (3) recycling of biogenic carbon into the deep mantle (Schulze et al. 2013; Walter et al. 2011; Thomson et al. 2014). Unfortunately, none of these models fully account for the widespread occurrence of light carbon in ophiolite-hosted diamonds. There is no clear evidence of a separate primordial reservoir of light carbon in the mantle and it is unlikely that such a feature would persist through several billions of years of mantle convection. Likewise, an unrealistic degree of fractionation of the main carbon reservoir would be required to produce the observed low values (Deines 2002). The only other known source of light carbon on Earth is biogenic material from Earth's crust, and recycling of such material currently appears to be the best explanation for its presence in ophiolites, particularly in light of the other evidence for subduction of oceanic crust outlined earlier. However, this model also has serious problems, including dehydration and potential melting of such material during subduction (Johnson and Plank 1999), dilution and oxidation of the carbonaceous component during metamorphism and deformation (Mathez et al. 1995), loss of sedimentary materials in the subducted slab due to gravitational instability during initial subduction (Kelemen and Manning 2015), and the coexistence of the isotopically heavy carbonate that comprises 25% of the ocean crust (Shilobreeva et al. 2011). Clearly, this problem needs additional study.

Always consult and cite the final, published document. See http:/www.minsocam.org or GeoscienceWorld

Nitrogen isotope variability in ophiolite-hosted diamonds

Nitrogen, which has a similar charge and ionic radius to carbon, is the most common impurity in diamonds (Cartigny 2005). The nitrogen isotopic compositions of crustal- and mantle-derived samples are distinct with mantle-derived peridotitic diamond (having an average value of –5 ± 4‰, Cartigny 2005), whereas the mean $\delta^{15}N$ value for crustal-derived samples is positive (e.g., pre-Cambrian crustal organic material = +6 ± 4‰) (Thomazo et al. 2009).

In our study, we found that the range of $\delta^{15}N$ values is significantly larger than the range of $\delta^{13}C$ values within ophiolite-hosted diamonds, with $\delta^{15}N$ values ranging from –12.9‰ to +25.5‰ (Table 1; Fig. 4). Thomassot et al. (2007) suggested that stable isotope fractionation during diamond formation in an open system could explain small variations in $\delta^{15}N$ values. However, it is highly unlikely that such a mechanism could account for the range of $\delta^{15}N$ observed in the Skenderbeu diamonds (Table 1; Fig. 4, Palot et al. 2012).

The Skenderbeu diamonds are also characterized by relatively low N contents, which range from 37 to 286 ppm (Table 1, Fig. 4). Such low contents of N do not appear to support the suggestion that the Skenderbeu diamonds originated from an ancient subducted plate, which presumably would be rich in nitrogen. Interestingly, single Skenderbeu diamonds may have both negative and positive $\delta^{15}N$ values, irrespective of the bulk $\delta^{13}C$ values and the nitrogen concentrations, for example, samples E184-9@1 and E184-9@2 (Table 1; Fig. 4). Hence, the nitrogen isotopic compositions and the nitrogen concentrations in these diamonds appear to be decoupled as has been suggested for diamonds in the Luobusa ophiolite of Tibet (Howell et al. 2015).

PROPOSED PETROGENETIC MODEL

Always consult and cite the final, published document. See http:/www.minsocam.org or GeoscienceWorld

Thus far, the diamonds in the Luobusa podiform chromitites, where ophiolite-hosted SuR-UHP minerals were first discovered, have been explained by mantle plumes, deep subduction or some combination of the two (Yang et al. 2014, 2015a; Zhou et al. 2014; McGowan et al. 2015; Robinson et al. 2015; Griffin et al. 2016). These models, however, are based on studies of the Luobusa and Ray-Iz ophiolite, which differ somewhat from the Mirdita ophiolite with respect to petrogenesis and geodynamic setting.

Here we present a conceptual model for the growth and exhumation of the Skenderbeu diamonds that can account for the data obtained during this study (Fig. 11). We emphasize that this model does not account for the array of other minerals reported in other ophiolites (Yang et al. 2014, 2015a, 2015b; Robinson et al. 2015) but it does focus on the geodynamic setting of the Skenderbeu massif as interpreted by Wu et al. (2018).

We propose that the carbon from which the diamonds formed was provided by recycled oceanic crust and lithosphere, but our data do not provide information on how the diamonds were brought back to the surface – instead we direct readers to previous comprehensive models for other ophiolites published by Yang et al. (2015a) and Griffin et al. (2016).

Despite that Mn-nodules do not have wide distribution at the ocean bottom (Verlaan et al. 2004), it is reasonable that a small portion of Mn-rich nodules and sediments were included in the subducting slab prior to formation of the ophiolite. Mn-Ni-Co-bearing material in the crust began to melt at approximately 1200°C, a temperature that can be reached easily in the upper mantle. The metal-bearing melts dissolved the other components of the nodules and the metasediments. With continuing subduction, the melts segregated into larger pools probably at depths greater than ~250 km where conditions are sufficiently reduced to stabilize the Mn-Ni-Co melt (Frost and McCammon 2008; Rohrbach et al. 2007, 2011). Under these conditions (the

Always consult and cite the final, published document. See http:/www.minsocam.org or GeoscienceWorld

exact depth is not known) the alloy melt can dissolve large amounts of carbon (Frost and McCammon 2008; Rohrbach and Schmidt 2011; Smith et al. 2016b), which is thought to be present as carbon-rich fluids. The presence of such fluids is documented in the fluid inclusions along the interface between the host diamond and the inclusion (Fig. 8b). During rapid uplift (McGowan et al. 2015; Howell et al. 2015; Griffin et al. 2016), when the buoyant material returns to the surface, oversaturation of carbon in the alloy melt is achieved and carbon is exsolved as diamond (P> ~ 5 GPa and T > ~ 1200°C, Stachel and Luth 2015). Note that crystallization of diamond from carbon-saturated, ultra-reduced fluids takes place quickly (Sokol et al. 2009), which may explain the small size of the ophiolite-hosted diamonds. During growth, the diamonds can occasionally include small part of the alloy melt (Fig. 8), producing inclusions like Ni-Mn-Co alloys, Ca-perovskite and potentially other minerals such as moissanite and coesite depending on the composition of the fluid released from the subducted slab. Further pressure release and temperature decrease allows the melt included in diamond to crystallize and the remaining fluid at the interface between alloy and diamond reacts with the alloy crystal, thus producing the corrosion we observed. Subsequently, the diamonds were overgrown by newly formed chromite and thus protected (e.g., Yang et al. 2014), and brought to the surface. The chromite grains may be incorporated into the peridotites and form chromitites in the mantle wedge (Robinson et al. 2015). The entire mass was then finally emplaced on land as the Skenderbeu massif during trench-continent collisions in the Late Jurassic (Wu et al. 2018).

Note that a rapid uplift from the diamond stability field is consistent with the low N-aggregation state, which has been used to argue against a long (geologically speaking) mantle residence (McGowan et al. 2015; Howell et al. 2015; Griffin et al. 2016) and protects the diamonds from resorption and/or oxidation after crystallization. McGowan et al. (2015) suggested that exhumation of deep mantle material in the fore-arc side of a subduction system is

Always consult and cite the final, published document. See http:/www.minsocam.org or GeoscienceWorld

a result of the initial steepening and subsequent rollback of the slab; this produces large-scale passive upwelling, which can rapidly develop into a self-maintaining, low-viscosity channel; this mechanism can allow the buoyant harzburgitic bodies that contain the diamonds to be rapidly (6-10 m.y.) excavated from the deep upper mantle or Transition Zone. This mechanism is consistent with the model proposed by Wu et al. (2018). In our model, the western and eastern Mirdita ophiolites record a progressive evolution from MORB to IAT and boninitic magmas within the same SSZ tectonic environment (i.e. arc-protoarc setting), which experienced rapid slab retreat during and after its initiation. We propose that rapid rollback of the slab triggered mantle ascent and that the Skenderbeu diamonds did not form from the alloy melt until the late stages of such rapid ascent (Fig. 11), which is compatible with their unusual N-aggregation characteristics (Howell et al. 2015).

The discovery of diamonds in the Mirdita ophiolite in the Western part of Neo-Tethys, as well as discoveries of diamonds in the Eastern part of Neo-Tethys and other tectonic belts implies a global occurrence of this new type of diamond. Ophiolite-hosted diamonds, like the Skenderbeu samples report here, provide a valuable and rare opportunity to study sublithospheric material that has been exhumed from the deep upper mantle and/or upper mantle transition zone. Thus, these diamonds provide a better understanding of deep cycling of the oceanic crust and the composition of the mantle.

ACKNOWLEDGMENTS

We thank our colleagues in CARMA and the Polytechnic University of Tirana (Albania) and in the Geological Survey of Albania for their assistance with the logistics of our fieldwork in the Skenderbeu massif. We also offer special thanks to Michael Wiedenbeck in the GFZ for his assistance with the SIMS analyses. Anja Schreiber (GFZ Potsdam) is thanked for the FIB foil

Always consult and cite the final, published document. See http:/www.minsocam.org or GeoscienceWorld

preparation. Paul T. Robinson (CUG), Qing Xiong (CUG), Yildirim Dilek (Miami University) are thanked for their highly constructive comments that helped to improve the paper. We thank the editor Paul Tomascak, reviewer Felix V. Kaminsky and an anonymous reviewer for their thorough and valuable comments that improved this manuscript. This research was funded by grants from the International Geoscience Programme (IGCP 649, 2015-2020), the National Natural Science Foundation of China (41541017, 41641015, 41720104009, 41520104003), and the project from the China Postdoctoral Science Foundation (2018M632942).

REFERENCES

Akaogi, M., Kawahara, A., Kojitani, H., Yoshida, K., Anwgawa, Y., and Ishii, T. (2018) High-pressure phase transitions in MgCr2O4-Mg2SiO4 composition: Reactions between olivine and chromite with implications for ultrahigh-pressure chromitites. American Mineralogist, 103, 161-170.

Arai, S., and Yurimoto, H. (1994) Podiform chromitites of the Tari-Misaka ultramafic complex, Southwestern Japan, as mantle melt interaction products. Economic Geology and the Bulletin of the Society of Economic Geologists, 89, 1279-1288.

Arai, S. (1997) Control of wall-rock composition on the formation of podiform chromitites as a result of magma/peridotite interaction. Resource Geology, 47, 177-188.

——— (2013) Conversion of low-pressure chromitites to ultrahigh-pressure chromitites by deep recycling: A good inference. Earth and Planetary Science Letters, 379, 81-87.

Bai, W.J., Zhou, M.F., and Robinson, P.T. (1993) Possibly diamond-bearing mantle peridotites and podiform chromitites in the Luobusa and Donqiao ophiolites, Tibet. Canadian Journal of Earth Sciences, 30, 1650-1659.

Ballhaus, C., Wirth, R., Fonseca, R.O.C., Blanchard, H., Pröll, W., Bragagni, A., Nagel, T.,

Always consult and cite the final, published document. See http:/www.minsocam.org or GeoscienceWorld

Schreiber, A., Dittrich, S., Thome, V., and others. (2017) Ultra-high pressure and ultra-reduced minerals in ophiolites may form by lightning strikes. Geochemical Perspectives Letter, 5, 42-46.

Ballhaus, C., Blanchard, H., Fonseca, R.O.C., and Bragagni, A. (2018) Reply 2 to comment on "Ultra-high pressure and ultra-reduced minerals in ophiolites may form by lightning strikes". Geochemical Perspectives Letter, 8, 8-10.

Beccaluva, L., Coltorti, M., Premti, I., Saccani, E., Siena, F.T., and Zeda, O. (1994) Mid-ocean ridge and supra-subduction affinities in the ophiolitic belts from Albania. Ofioliti, 19, 77-96.

Bulanova, G.P., Walter, M.J., Smith, C.B., Kohn, S.C., Armstrong, L.S., Blundy, J., and Gobbo, L. (2010) Mineral inclusions in sublithospheric diamonds from Collier 4 kimberlite pipe, Juina, Brazil: subducted protoliths, carbonated melts and primary kimberlite magmatism. Contributions to Mineralogy and Petrology, 160, 489-510.

Caracas, R., and Wentzcovitch, R.M. (2006) Theoretical determination of the structures of CaSiO3 perovskites. Acta Crystallographica, 62, 1025-1030.

Cartigny, P., Harris, J.W., and Javoy, M. (1998) Eclogitic Diamond Formation at Jwaneng: No Room for a Recycled Component. Science, 280, 1421-1424.

Cartigny, P. (2005) Stable isotopes and the origin of diamond. Elements, 1, 79-84.

Chiari, M., Marcucci, M., and Prela, M. (2004) Radiolarian assemblages from the Jurassic cherts of Albania: New data. Ofioliti, 29, 95-105.

Das, S., Mukherjee, B.K., Basu, A.R., and Sen, K. (2015) Peridotitic minerals of the Nidar Ophiolite in the NW Himalaya: sourced from the depth of the mantle transition zone and above. Geological Society London Special Publications, 412, 271-286.

Das, S., Basu, A.R., and Mukherjee, B.K. (2017) In situ peridotitic diamond in Indus ophiolite sourced from hydrocarbon fluids in the mantle transition zone. Geology, 45, 755-758.

Always consult and cite the final, published document. See http:/www.minsocam.org or GeoscienceWorld

Deines, P. (2002) The carbon isotope geochemistry of mantle xenoliths. Earth-Science Reviews, 58, 247-278.

Dilek, Y. (2003) Ophiolite concept and its evolution. In Y. Dilek, and S. Newcomb, Ed., Ophiolite concept and the evolution of geological thought, p. 1-16. Geological Society of America Special Papers 373, Boulder, Colorado.

Dilek, Y., and Flower, M.F.J. (2003) Arc-trench rollback and forearc accretion: 2. A model template for ophiolites in Albania, Cyprus, and Oman. Special Publication-Geological Society of London, 218, 43-68.

Dilek, Y., Shallo, M., and Furnes, H. (2005) Rift-drift, seafloor spreading, and subduction tectonics of Albanian ophiolites. International Geology Review, 47, 147-176.

Dilek, Y., Furnes, H., and Shallo, M. (2008) Geochemistry of the Jurassic Mirdita Ophiolite (Albania) and the MORB to SSZ evolution of a marginal basin oceanic crust. Lithos, 100, 174-209.

Dilek, Y., and Morishita, T. (2009) Melt migration and upper mantle evolution during incipient arc construction: Jurassic Eastern Mirdita ophiolite, Albania. Island Arc, 18, 551-554.

Dobrzhinetskaya, L.F., Green, H.W.I., Mitchell, T.E., and Dickerson, R.M. (2001) Metamorphic diamonds: Mechanism of growth and inclusion of oxides. Geology, 29, 263-266.

Dobrzhinetskaya, L.F., Green, H.W., Bozhilov, K.N., Mitchell, T.E., and Dickerson, R.M. (2003a) Crystallization environment of Kazakhstan microdiamond: evidence from nanometric inclusions and mineral associations. Journal of Metamorphic Geology, 21, 425–437.

Dobrzhinetskaya, L.F., Green, H.W., Weschler, M., Darus, M., Wang, Y.C., Massonne, H.J., and Stöckhert, B. (2003b) Focused ion beam technique and transmission electron microscope studies of microdiamonds from the Saxonian Erzgebirge, Germany. Earth and Planetary

Always consult and cite the final, published document. See http:/www.minsocam.org or GeoscienceWorld

Science Letters, 210, 399-410.

Dobrzhinetskaya, L.F., Wirth, R., Yang, J.S., Hutcheon, I.D., Weber, P.K., and Green, H.W. (2009) High-pressure highly reduced nitrides and oxides from chromitite of a Tibetan ophiolite. Proceedings of the National Academy of Sciences, 106, 19233-19238.

Dobrzhinetskaya, L.F., Ii, H.W.G., Takahata, N., Sano, Y., and Shirai, K. (2010) Crustal Signature of δ13C and Nitrogen Content in Microdiamonds from Erzgebirge,Germany: Ion Microprobe Studies. Journal of Earth Science, 21, 623-634.

Dobrzhinetskaya, L.F. (2012) Microdiamonds—frontier of ultrahigh-pressure metamorphism: a review. Gondwana Research, 21, 207-223.

Egerton, R.F., and Whelan, M.J. (1974) Electron energy loss spectra of diamond, graphite and amorphous carbon. Journal of Electron Spectroscopy & Related Phenomena, 3, 232-236.

Frasheri, A., Nishani, P., Bushati, S., and Hyseni, A. (1996) Relationship between tectonic zones of the Albanides, based on results of geophysical studies. In A.P. Ziegler, and F. Horwath, Ed., Peri-Tethys Memoir 2: Structure and prospects of Alpine basins and forelands, p. 485-511. Memoire Musée Historique de Paris.

Frost, D.J., and Mccammon, C.A. (2008) The Redox State of Earth's Mantle. Annual Review of Earth & Planetary Sciences, 36, 389-420.

Fujino, K., Suzuki, K., Hamane, D., Seto, Y., Nagai, T., and Sata, N. (2008) High-pressure phase relation of $MnSiO_3$ up to 85 GPa: Existence of $MnSiO_3$ perovskite. American Mineralogist, 93, 653-657.

Galuskin, E.V., Gfeller, F., Armbruster, T., Galuskina, I.O., Vapnik, Y., Murashko, M., and Dzierżanowski, P. (2013) New minerals and nomenclature modifications approved in 2013. Mineralogical Magazine, 77, 2695-2709.

Garvie, L.A.J., Buseck, P.R., and Craven, A.J. (1995) Electron-loss near-edge structure (ELNES)

Always consult and cite the final, published document. See http:/www.minsocam.org or GeoscienceWorld

as a probe of valence and coordination number. Canadian Mineralogist, 33, 1157-1166.

Gokcen, N.A. (1991) The Mn-Ni (Manganese-Nickel) System. Journal of Phase Equilibria, 12, 313-321.

Golovko, A.V., and Kaminsky, F.V. (2010) The Shoshonite-Absarokite-Picrite Karashoho Pipe, Uzbekistan: An Unusual Diamond Deposit in an Atypical Tectonic Environment. Economic Geology, 105, 825-840.

Goresy, A.E., Gillet, P., Chen, M., Künstler, F., Graup, G., and Stähle, V. (2001) In situ discovery of shock-induced graphite-diamond phase transition in gneisses from the Ries Crater, Germany. American Mineralogist, 86, 611-621.

Griffin, W.L., Afonso, J.C., Belousova, E.A., Gain, S.E., Gong, X.H., Gonzalez-Jimenez, J.M., Howell, D., Huang, J.X., McGowan, N., Pearson, N.J., and others. (2016) Mantle Recycling: Transition Zone Metamorphism of Tibetan Ophiolitic Peridotites and its Tectonic Implications. Journal of Petrology, 57, 655-684.

Guo, C.P., and Du, Z.M. (2005) Thermodynamic optimization of the Mn–Ni system. Intermetallics, 13, 525-534.

Gupta, K.P. (1999) The Co-Mn-Ni (Cobalt-Manganese-Nickel) system. Journal of Phase Equilibria, 20, 527-532.

Haggerty, S.E. (2017) Carbonado diamond: A review of properties and origin. Gems & Gemology, 53, 168-179.

Harte, B. (2010) Diamond formation in the deep mantle: the record of mineral inclusions and their distribution in relation to mantle dehydration zones. Mineralogical Magazine, 74, 189-215.

Hoeck, V., Koller, F., Meisel, T., Onuzi, K., and Kneringer, E. (2002) The Jurassic South Albanian ophiolites: MOR- vs. SSZ-type ophiolites. Lithos, 65, 143-164.

Always consult and cite the final, published document. See http:/www.minsocam.org or GeoscienceWorld

Howell, D., Griffin, W.L., Yang, J.S., Gain, S., Stern, R.A., Huang, J.X., Jacob, D.E., Xu, X.Z., Stokes, A.J., and O'Reilly, S.Y. (2015) Diamonds in ophiolites: Contamination or a new diamond growth environment? Earth and Planetary Science Letters, 430, 284-295.

Hoxha, M., and Boullier, A.M. (1995) The peridotites of the Kukes ophiolite (Albania) - structure and kinematics. Tectonophysics, 249, 217-231.

Huang, Z., Yang, J.S., Robinson, P.T., Zhu, Y.W., Xiong, F.H., Liu, Z., Zhang, Z.M., and Xu, W. (2015) The Discovery of Diamonds in Chromitites of the Hegenshan Ophiolite, Inner Mongolia, China. Acta Geologica Sinica (English Edition), 89, 341-350.

Hull, D., and Bacon, D.J. (2011) Introduction to Dislocations (Fifth Edition), 257 p. Elsevier Butterworth-Heinemann, Oxford.

Jablon, B.M., and Navon, O. (2016) Most diamonds were created equal. Earth and Planetary Science Letters, 443, 41-47.

Jacob, D.E., Kronz, A., and Viljoen, K.S. (2004) Cohenite and native iron inclusions in garnets from polycrystalline diamonds. Contribution to Mineralogy and Petrology, 146, 566-576.

Johnson, M.C., and Plank, T. (1999) Dehydration and melting experiments constrain the fate of subducted sediments. Geochemistry Geophysics Geosystems, 1, 597-597.

Jung, D.Y., and Oganov, A.R. (2005) Ab initio study of the high-pressure behavior of CaSiO3 perovskite. Physics & Chemistry of Minerals, 32, 146-153.

Kaminsky, F.V. (2007) Non-kimberlitic diamondiferous igneous rocks: 25 years after. Journal of the Geological Society of India, 259, 557-575.

Kaminsky, F.V., and Wirth, R. (2011) Iron carbide inclusions in lower-mantle diamond from Juina, Brazil. Canadian Mineralogist, 49, 555-572.

Kaminsky, F.V., Wirth, R., Anikin, L.P., Morales, L., and Schreiber, A. (2016) Carbonado-like diamond from the Avacha active volcano in Kamchatka, Russia. Lithos, 265, 222-236.

Always consult and cite the final, published document. See http:/www.minsocam.org or GeoscienceWorld

Kaminsky, F.V. (2017) The Earth's Lower Mantle, 340 p. Springer Geology, Switzerland.

Kasten, S., Glasby, G.P., Schulz, H.D., Friedrich, G., and Andreev, S.I. (1998) Rare earth elements in manganese nodules from the South Atlantic Ocean as indicators of oceanic bottom water flow. Marine Geology, 146, 33-52.

Katrinak, K.A., Rez, P., and Buseck, P.R. (1992) Structural variations in individual carbonaceous particles from an urban aerosol. Environmental Science & Technology, 26, 1967-1976.

Kelemen, P.B., and Manning, C.E. (2015) Reevaluating carbon fluxes in subduction zones, what goes down, mostly comes up. Proceedings of the National Academy of Sciences of the United States of America, 112, 3997-4006.

Koeberl, C., Masaitis, V.L., Shafranovsky, G.I., Gilmour, I., Langenhorst, F., and Schrauder, M. (1995) Diamonds from the Popigai impact structure, Russia. Geology, 25, 967-970.

Koller, F., Hoeck, V., Meisel, T., Ionescu, C., Onuzi, K., and Ghega, D. (2006) Cumulates and gabbros in southern Albanian ophiolites: their bearing on regional tectonic setting. Geological Society London Special Publications, 260, 267-299.

Kurata, H., Lefèvre, E., Colliex, C., and Brydson, R. (1993) Electron Energy-Loss Near-Edge Structure in the Oxygen K-Edge Spectra of Transition-Metal Oxides. Physical Review B Condensed Matter, 47, 13763-13768.

Leinenweber, K., Utsumi, W., Tsuchida, Y., Yagi, T., and Kurita, K. (1991) Unquenchable high-pressure perovskite polymorphs of MnSnO3 and FeTiO3. Physics and Chemistry of Minerals, 18, 244-250.

Li, L., Weidner, D.J., Brodholt, J., Alfe, D., Price, G.D., Caracas, R., and Wentzcovitch, R. (2006) Phase stability of CaSiO3 perovskite at high pressure and temperature: Insights from ab initio molecular dynamics. Physics of the Earth & Planetary Interiors, 155, 260-268.

Li, L., Nagai, T., Seto, Y., Fujino, K., Kawano, J., and Itoh, S. (2015) Superior solid solubility of

Always consult and cite the final, published document. See http:/www.minsocam.org or GeoscienceWorld

$MnSiO_3$ in $CaSiO_3$ perovskite. Physics & Chemistry of Minerals, 42, 123-129.

Lian, D.Y., Yang, J.S., Dilek, Y., Wu, W.W., Zhang, Z.M., Xiong, F.H., Liu, F., and Zhou, W.D. (2017) Diamond, Moissanite and other unusual minerals in podiform chromitites from the Pozanti-karsanti ophiolite, southern Turkey: implication for the deep mantle origin and ultra-reducing conditions in podiform chromitite. American Mineralogist, 102, 1101-1113.

Lian, D.Y., Yang, J.S., Wiedenbeck, M., Dilek, Y., Rocholl, A., and Wu, W.W. (2018) Carbon and nitrogen isotope, and mineral inclusion studies on the diamonds from the Pozanti–Karsanti chromitite, Turkey. Contributions to Mineralogy and Petrology, 173, 72.

Liang, F.H., Xu, Z.Q., and Zhao, J. (2014) In-situ Moissanite in Dunite: Deep Mantle Origin of Mantle Peridotite in Luobusa Ophiolite, Tibet. Acta Geologica Sinica (English Edition), 88, 517-529.

Litvin, Y.A., Litvin, V.Y., and Kadik, A.A. (2008) Experimental characterization of diamond crystallization in melts of mantle silicate-carbonate-carbon systems at 7.0–8.5 GPa. Geochemistry International, 46, 531-553.

Mathez, E.A., Fogel, R.A., Hutcheon, I.D., and Marshintsev, V.K. (1995) Carbon isotopic composition and origin of SiC from kimberlites of Yakutia, Russia. Geochimica et Cosmochimica Acta, 59, 781-791.

McGowan, N.M., Griffin, W.L., González-Jiménez, J.M., Belousova, E., Afonso, J.C., Shi, R.D., McCammon, C.A., Pearson, N.J., and O Reilly, S.Y. (2015) Tibetan chromitites: Excavating the slab graveyard. Geology, 43, 179-182.

Mikhail, S., Dobosi, G., Verchovsky, A.B., Kurat, G., and Jones, A.P. (2013) Peridotitic and websteritic diamondites provide new information regarding mantle melting and metasomatism induced through the subduction of crustal volatiles. Geochimica et Cosmochimica Acta, 107(3), 1-11.

Always consult and cite the final, published document. See http:/www.minsocam.org or GeoscienceWorld

Moe, K.S., Yang, J.S., Johnson, P., Xu, X.Z., and Wang, W.Y. (2018) Spectroscopic analysis of microdiamonds in ophiolitic chromitite and peridotite. Lithosphere, 10, 133-141.

Moresi, L., Betts, P.G., Miller, M.S., and Cayley, R.A. (2014) Dynamics of continental accretion. Nature, 508, 245-248.

Palot, M., Cartigny, P., Harris, J.W., Kaminsky, F.V., and Stachel, T. (2012) Evidence for deep mantle convection and primordial heterogeneity from nitrogen and carbon stable isotopes in diamond. Earth and Planetary Science Letters, 357, 179-193.

Pearson, D.G., Davies, G.R., Nixon, P.H., and Milledge, H.J. (1989) Graphitized diamonds from a peridotite massif in Morocco and implications for anomalous diamond occurrences. Nature, 338, 60-62.

Robinson, P.T., Bai, W.J., Malpas, J., Yang, J.S., Zhou, M.F., Fang, Q.S., Hu, X.F., Cameron, S., and Staudigel, H. (2004) Ultrahigh-pressure minerals in the Luobusa Ophiolite, Tibet, and their tectonic implications. Special Publication-Geological Society of London, 226, 247-272.

Robinson, P.T., Trumbull, R.B., Schmitt, A., Yang, J.S., Li, J.W., Zhou, M.F., Erzinger, J., Dare, S., and Xiong, F.H. (2015) The origin and significance of crustal minerals in ophiolitic chromitites and peridotites. Gondwana Research, 27, 486-506.

Rohrbach, A., Ballhaus, C., Golla Schindler, U., Ulmer, P., Kamenetsky, V.S., and Kuzmin, D.V. (2007) Metal saturation in the upper mantle. Nature, 449, 456-458.

Rohrbach, A., and Schmidt, M.W. (2011) Redox freezing and melting in the Earth's deep mantle resulting from carbon-iron redox coupling. Nature, 472, 209-12.

Rohrbach, A., Ballhaus, C., Ulmer, P., Gollaschindler, U., and Schönbohm, D. (2011) Experimental Evidence for a Reduced Metal-saturated Upper Mantle. Journal of Petrology, 52, 717-731.

Saccani, E., and Photiades, A. (2004) Mid-ocean ridge and supra-subduction affinities in the

Always consult and cite the final, published document. See http:/www.minsocam.org or GeoscienceWorld

Pindos ophiolites (Greece): implications for magma genesis in a forearc setting. Lithos, 73, 229-253.

Saccani, E., and Tassinari, R. (2015) The role of MORB and SSZ magma-Types in the formation of Jurassic ultramafic cumulates in the Mirdita ophiolites (Albania) as deduced from chromian spinel and olivine chemistry. Ofioliti, 40, 37-56.

Schulze, D.J., Harte, B., Page, F.Z., Valley, J.W., Channer, D.M.D., and Jaques, A.L. (2013) Anticorrelation between low 13C of eclogitic diamonds and high 18O of their coesite and garnet inclusions requires a subduction origin. Geology, 41, 455-458.

Shallo, M., Kodra, A., and Gjata, K. (1990) Geotectonics of the Albanian ophiolites. Ophiolites: Oceanic Crustal Analogues. The Geological Survey Department, Cyprus, 265-270.

Shallo, M., and Dilek, Y. (2003) Development of the ideas on the origin of Albanian ophiolites. Special Papers-Geological Society of America, 351-364.

Shenjatari, A., and Beqiraj, A. (2010) Petrogenesis of Skenderbeu Peridotites (Western Ophiolitic Belt, Albania). Journal of International Environmental Application and Science, 10, 470-479.

Shilobreeva, S., Martinez, I., Busigny, V., Agrinier, P., and Laverne, C. (2011) Insights into C and H storage in the altered oceanic crust: Results from ODP/IODP Hole 1256D. Geochimica et Cosmochimica Acta, 75, 2237-2255.

Shirey, S.B., Cartigny, P., Frost, D.J., Keshav, S., Nestola, F., Nimis, P., Pearson, D.G., Sobolev, N.V., and Walter, M.J. (2013) Diamonds and the geology of mantle carbon. Reviews of Mineral Geochemistry, 75, 355-421.

Smart, K.A., Chacko, T., Stachel, T., Muehlenbachs, K., Stern, R.A., and Heaman, L.M. (2011) Diamond growth from oxidized carbon sources beneath the Northern Slave Craton, Canada: A δ 13 C–N study of eclogite-hosted diamonds from the Jericho kimberlite. Geochimica et

Always consult and cite the final, published document. See http:/www.minsocam.org or GeoscienceWorld

Cosmochimica Acta, 75, 6027-6047.

Smith, C.B., Walter, M.J., Bulanova, G.P., Mikhail, S., Burnham, A.D., Gobbo, L., and Kohn, S.C. (2016a) Diamonds from Dachine, French Guiana: a unique record of Early Proterozoic subduction. Lithos, 265, 82-95.

Smith, E.M., Kopylova, M.G., Frezzotti, M.L., and Afanasiev, V.P. (2015) Fluid inclusions in Ebelyakh diamonds: Evidence of CO2 liberation in eclogite and the effect of H2O on diamond habit. Lithos, s 216–217, 106-117.

Smith, E.M., and Wang, W.Y. (2016) Fluid CH4 and H2 trapped around metallic inclusions in HPHT synthetic diamond. Diamond & Related Materials, 68, 10-12.

Smith, E.M., Shirey, S.B., Nestola, F., Bullock, E.S., Wang, J.H., Richardson, S.H., and Wang, W.Y. (2016b) Large gem diamonds from metallic liquid in Earth's deep mantle. Science, 354, 1403-1405.

Sobolev, N.V., and Shatsky, V.S. (1990) Diamond inclusions in garnets from metamorphic rocks: a new environment for diamond formation. Nature, 343, 742-746.

Sobolev, N.V., Kaminsky, F.V., Griffin, W.L., Yefimova, E.S., Win, T.T., Ryan, C.G., and Botkunov, A.I. (1997) Mineral inclusions in diamonds from the Sputnik kimberlite pipe, Yakutia. Lithos, 39, 135-157.

Sokol, A.G., Palyanova, G.A., Palyanov, Y.N., Tomilenko, A.A., and Melenevsky, V.N. (2009) Fluid regime and diamond formation in the reduced mantle: Experimental constraints. Geochimica et Cosmochimica Acta, 73, 5820-5834.

Stachel, T. (2001) Diamonds from the asthenosphere and the transition zone. European Journal of Mineralogy, 13, 883-892.

Stachel, T., Brey, G.P., and Harris, J.W. (2005) Inclusions in sublithospheric diamonds: glimpses of deep Earth. Elements, 1, 73-78.

Always consult and cite the final, published document. See http:/www.minsocam.org or GeoscienceWorld

Stachel, T., and Harris, J.W. (2008) The origin of cratonic diamonds—constraints from mineral inclusions. Ore Geology Reviews, 34, 5-32.

Stachel, T., and Luth, R.W. (2015) Diamond Formation – Where, when and how? Lithos, 220-223, 200-220.

Taylor, W.R., and Green, D.H. (1989) The role of reduced C-O-H fluids in mantle partial melting. In J. Ross, Ed., Kimberlites and related rocks, p. 592-602. Blackwell Scientific Publications, Australia.

Thomassot, E., Cartigny, P., Harris, J.W., and Viljoen, K.S. (2007) Methane-related diamond crystallization in the Earth's mantle: stable isotope evidences from a single diamond-bearing xenolith. Earth and Planetary Science Letters, 257, 362-371.

Thomazo, C., Pinti, D.L., Busigny, V., Ader, M., Hashizume, K., and Philippot, P. (2009) Biological activity and the Earth's surface evolution: Insights from carbon, sulfur, nitrogen and iron stable isotopes in the rock record. Comptes Rendus Palevolcanism, 8, 665-678.

Thomson, A.R., Kohn, S.C., Bulanova, G.P., Smith, C.B., Araujo, D., and Walter, M.J. (2014) Origin of sub-lithospheric diamonds from the Juina-5 kimberlite (Brazil): constraints from carbon isotopes and inclusion compositions. Contributions to Mineralogy and Petrology, 168, 1081.

Verlaan, P.A., Cronan, D.S., and Morgan, C.L. (2004) A comparative analysis of compositional variations in and between marine ferromanganese nodules and crusts in the South Pacific and their environmental controls. Progress in Oceanography, 63, 125-158.

Walter, M.J., Kohn, S.C., Araujo, D., Bulanova, G.P., Smith, C.B., Gaillou, E., Wang, J., Steele, A., and Shirey, S.B. (2011) Deep Mantle Cycling of Oceanic Crust: Evidence from diamonds and their mineral inclusions. Science, 334, 54-57.

Wirth, R. (2004) Focused Ion Beam (FIB): A novel technology for advanced application of

Always consult and cite the final, published document. See http:/www.minsocam.org or GeoscienceWorld

micro- and nanoanalysis in geosciences and applied mineralogy. European Journal of Mineralogy, 16, 863-876.

——— (2009) Focused Ion Beam (FIB) combined with SEM and TEM: Advanced analytical tools for studies of chemical composition, microstructure and crystal structure in geomaterials on a nanometre scale. Chemical Geology, 261, 217-229.

Wu, W.W., Yang, J.S., Ma, C.Q., Milushi, I., Lian, D.Y., and Tian, Y.Z. (2017) Discovery and Significance of Diamonds and Moissanites in Chromitite within the Skenderbeu Massif of the Mirdita Zone Ophiolite, West Albania. Acta Geologica Sinica (English Edition), 91, 882-897.

Wu, W.W., Yang, J.S., Dilek, Y., Milushi, I., and Lian, D.Y. (2018) Multiple episodes of melting, depletion, and enrichment of the Tethyan mantle: Petrogenesis of the peridotites and chromitites in the Jurassic Skenderbeu massif, Mirdita ophiolite, Albania. Lithosphere, 10, 54-78.

Xhomo, A., Kodra, A., and Dimo, L. (2002) Geological Map of Albania 1: 200,000 scale. Geological Survey of Albania.

Xiong, F.H., Yang, J.S., Robinson, P.T., Dilek, Y., Milushi, I., Xu, X.Z., Zhou, W.D., Zhang, Z.M., and Rong, H. (2017) Diamonds Discovered from High–Cr Podiform Chromitites of Bulqiza, Eastern Mirdita Ophiolite, Albania. Acta Geologica Sinica (English Edition), 91, 455–468.

Xu, S.T., Okay, A.I., Ji, S.Y., Sengör, A.M.C., Wen, S., Liu, Y.C., and Jiang, L.L. (1992) Diamond from the Dabie Shan Metamorphic Rocks and Its Implication for Tectonic Setting. Science, 256, 80-82.

Xu, X.Z., Yang, J.S., Chen, S.Y., Fang, Q.S., Bai, W.J., and Ba, D.Z. (2009) Unusual mantle mineral group from chromitite orebody Cr-11 in Luobusa ophiolite of Yarlung-Zangbo

Always consult and cite the final, published document. See http:/www.minsocam.org or GeoscienceWorld

suture zone, Tibet. Journal of Earth Science, 20, 284-302.

Xu, X.Z., Yang, J.S., Robinson, P.T., Xiong, F.H., Ba, D.Z., and Guo, G.L. (2015) Origin of ultrahigh pressure and highly reduced minerals in podiform chromitites and associated mantle peridotites of the Luobusa ophiolite, Tibet. Gondwana Research, 27, 686-700.

Yamamoto, S., Komiya, T., Hirose, K., and Maruyama, S. (2009) Coesite and clinopyroxene exsolution lamellae in chromites: In-situ ultrahigh-pressure evidence from podiform chromitites in the Luobusa ophiolite, southern Tibet. Lithos, 109, 314-322.

Yang, J.S., Dobrzhinetskaya, L., Bai, W.J., Fang, Q.S., Robinson, P.T., Zhang, J., and Green, H.W. (2007) Diamond-and coesite-bearing chromitites from the Luobusa ophiolite, Tibet. Geology, 35, 875-878.

Yang, J.S., Robinson, P.T., and Dilek, Y. (2014) Diamonds in ophiolites. Elements, 10, 127-130.

Yang, J.S., Meng, F.C., Xu, X.Z., Robinson, P.T., Dilek, Y., Makeyev, A.B., Wirth, R., Wiedenbeck, M., Griffin, W.L., and Cliff, J. (2015a) Diamonds, native elements and metal alloys from chromitites of the Ray-Iz ophiolite of the Polar Urals. Gondwana Research, 27, 459-485.

Yang, J.S., Robinson, P.T., and Dilek, Y. (2015b) Diamond-bearing ophiolites and their geological occurrence. Episodes, 38, 344-364.

Yang, J.S., Trumbull, R.B., Robinson, P.T., Xiong, F.H., and Lian, D.Y. (2018) Comment 2 on "Ultra-high pressure and ultra-reduced minerals in ophiolites may form by lightning strikes". Geochemical Perspectives Letter, 8, 6-7.

Zhang, R.Y., Yang, J.S., Ernst, W.G., Jahn, B.M., Iizuka, Y., and Guo, G.L. (2016) Discovery of in situ super-reducing, ultrahigh-pressure phases in the Luobusa ophiolitic chromitites, Tibet: new insights into the deep upper mantle and mantle transition zone. American Mineralogist, 101, 1245-1251.

Always consult and cite the final, published document. See http:/www.minsocam.org or GeoscienceWorld

Zhang, Y.F., Jin, Z.M., Griffin, W.L., Wang, C., and Wu, Y. (2017) High-pressure experiments provide insights into the Mantle Transition Zone history of chromitite in Tibetan ophiolites. Earth and Planetary Science Letters, 463, 151-158.

Zhou, M.F., Robinson, P.T., and Bai, W.J. (1994) Formation of podiform chromitites by melt/rock interaction in the upper mantle. Mineralium Deposita, 29, 98-101.

Zhou, M.F., Robinson, P.T., Su, B.X., Gao, J.F., Li, J.W., Yang, J.S., and Malpas, J. (2014) Compositions of chromite, associated minerals, and parental magmas of podiform chromite deposits: The role of slab contamination of asthenospheric melts in suprasubduction zone environments. Gondwana Research, 26, 262-283.

Figure Captions

FIGURE 1. (**a**) Distribution of major Tethyan ophiolites and suture zones in the Mediterranean region (modified from Dilek and Flower 2003). DSF: Dead Sea Fault; EAF: East Anatolian Fault; NAF: North Anatolian Fault; BZCZ: Bitlis Zagros Collision Zone. (**b**) Simplified geological map of the Internal Albanides, showing the Mirdita zone ophiolites and major peridotite massifs, the conjugate passive margins of Apulia and Pelagonia-Korabi, and the Cenozoic sedimentary basins (modified from Dilek et al. 2005, 2008).

FIGURE 2. Schematic geological map of the Skenderbeu massif (modified from Xhomo et al. 2002).

FIGURE 3. Images showing diamonds recovered from the Skenderbeu chromitite. (**a**) Photomicrograph showing abundant light yellow to yellow diamonds. (**b**) SEM image of an irregular diamond grain. (**c**) SEM image of a subhedral diamond. (**d**) Raman spectrogram showing the typical Raman shift for diamond around 1325 cm^{-1}.

Always consult and cite the final, published document. See http:/www.minsocam.org or GeoscienceWorld

FIGURE 4. Cathodoluminescence (CL) images of twelve diamonds from the Skenderbeu massif, showing the locations of SIMS analyses for carbon isotopes (yellow spots, ‰), nitrogen isotopes (red spots, ‰), and N concentrations (ppm) (Table 1).

FIGURE 5. (**a**) $\delta^{15}N_{AIR}$ vs $\delta^{13}C_{PDB}$ plot of isotopic compositions of the Skenderbeu diamonds compared to other global sources of mantle diamond. Skenderbeu data from this study are shown as filled squares and the data from Howell et al. (2015) are shown as filled circles. The compositional separation shows that ophiolite-hosted diamonds and other Earth diamonds are unrelated. The comparative fields for peridotitic (olivine, clinopyroxene, and orthopyroxene), eclogitic (garnet and clinopyroxene), transitional types and fibrous diamonds are from a global database sourced from Haggerty (2017) and references therein. Data for the mantle mean are from Cartigny (2005). OCT: octahedral growth sector of the diamonds. CUB: cubic growth sector of the diamonds. (**b**) $\delta^{15}N_{AIR}$ vs N concentrations of the Skenderbeu diamonds. The data from both sectors of the ophiolite-hosted diamonds show a negative relationship, with increasing $\delta^{15}N_{AIR}$ as nitrogen concentrations decrease.

FIGURE 6. TEM images of foil E180-1#5006. (**a**) High-angle annular dark field (HAADF) image of the entire foil. The bright layer on bottom of the foil is a platinum protection layer for FIB milling. The foil rests partially on a perforated thin (<10 nm) carbon film. (**b**) HAADF image of inclusion 1. The bright contrasted areas within the inclusion are Si-based with an admixture of Mg, Al, and Fe. The absence of any diffraction contrast suggests an amorphous state of the silicate material. The matrix material of the inclusion is C with some admixture of Cl and S. (**c**) HAADF image of inclusion no. 2 (grey ellipse areas are caused by the carbon film). (**d**) Dislocations in Skenderbeu diamond E180-1. The dislocation lines are preferentially straight and typically steeply inclined relative to the foil surface.

Always consult and cite the final, published document. See http:/www.minsocam.org or GeoscienceWorld

FIGURE 7. EDX spectra of regions of interest (blue boxes in Fig. 6) in diamond inclusions. **(a)** and **(b)** inclusion 1 data from box 1 and 2, respectively. **(c)**, **(d)**, and **(e)** inclusion 2 data from box 1, 2, and 3, respectively. Gallium peaks are artifacts of FIB preparation and Cu peaks are from the copper grid. Particularly large C peaks are from some combination of the host diamond and amorphous C in the inclusions.

FIGURE 8. TEM images of foil E180-5#5010 with details as in Fig. 6. **(a)** HAADF image of the entire foil showing the location of inclusion 3. **(b)** HAADF image of inclusion 3, which is composed of perovskite, NiMnCo alloy, and fluid. Dark areas represent pores that may have formed during preparation of the foil. **(c)** Dislocations in Skenderbeu diamond E180-5.

FIGURE 9. (**a**) EDX spectrum of the perovskite in inclusion 3 as shown in Fig. 8b. (**b**) EDX spectrum of the NiMnCo alloy in inclusion 3 as indicated in Fig. 8b. (**c**) and (**d**) EDX spectra of the fluid indicated by the two blue arrows in Fig. 8b. The fluid contains mainly Mg, K and Cl; the other element peaks may be from the adjacent perovskite and the NiMnCo alloy. The Ga peaks are from preparation of the foil and the Cu peaks are from the copper grid.

FIGURE 10. (**a**) Energy-filtered high-resolution image of perovskite in inclusion 3. (**b**) Calculated diffraction pattern (fast Fourier transform, FFT) of the same nano-crystal.

FIGURE 11. Model of Skenderbeu diamond formation. (**a**) Top right shows organic carbon ($\delta^{13}C \sim -25$ ‰, Shilobreeva et al. 2011) and Mn (Kasten et al. 1998 and references therein) are added to the subducting slab. Subduction carries this oceanic crustal assemblage past sub-arc depths until stagnated in the transition zone. This may cause partial melting of the slab and the formation of alloy melts. Metal segregation may be aided by deformation of the subducting slab in the transition zone. The metal composition of the melt evolves to Ni-Mn-Co. Carbon saturation is achieved by assimilating further C. (**b**) Arrival and rapid rollback of a new

Always consult and cite the final, published document. See http:/www.minsocam.org or GeoscienceWorld

slab (Wu et al. 2018) promotes broad mantle upwelling (Moresi et al. 2014), which rapidly develops into channelized upwelling that can carry buoyant material up from the transition zone to shallow depths in 7-10 m. y. (Howell et al. 2015; McGowan et al. 2015; Griffin et al. 2016**).** During rapid uplift, when the buoyant material including the alloy melt saturated with C returns to the shallow depths, C is exsolved as diamond. Diamonds start growing and can collect sparse inclusions, including some of the alloy melt and some of the high-density fluid. Eventually, the Skenderbeu diamonds are incorporated into the Skenderbeu massif. The geodynamic model of the Skenderbeu massif, Mirdita ophiolite in (b) is based on Wu et al. (2018). WMO: western Mirdita ophiolite; EMO: eastern Mirdita ophiolite; CLM: continental lithosphere mantle; OLM: oceanic lithosphere mantle; CC: continental crust; OC: oceanic crust; AP: accretion prism; MORB: mid-oceanic ridge basalt. See text for discussion.

FIGURE A1. (a) Electron energy-loss spectrum (EELS) showing the O K-edge of inclusion 2. **(b)** and **(c)** EELS spectra showing the C K-edge of the inclusions 1 and 2, respectively. The broad, featureless σ* peak, indicating many randomly oriented bonding configurations, is typical of amorphous material.

APPENDIX

Analytical techniques are available at the appendix.

The presence of O in inclusion 1, the presence of amorphous C in inclusions 1 and 2 indicated by EELS maps that are shown in Fig. A1.

Always consult and cite the final, published document. See http:/www.minsocam.org or GeoscienceWorld

Table 1. Carbon, nitrogen isotopic compositions and 1 sd (standard deviation) of Skenderbeu diamonds.

Analysis Name	$\delta^{13}C_{PDB}$ (‰)	1 sd (‰)	$\delta^{15}N_{AIR}$ (‰)	1 sd (‰)	N content (ppm)	1 sd (ppm)	CL image
E180-3@1	-26.7	0.05	N.A.	N.A.	N.A.	N.A.	Bright
E180-4@1	-25.7	0.04	0.4	1.57	235.8	0.86	Bright
E180-4@2	-26.4	0.03	N.A.	N.A.	N.A.	N.A.	Dark
E180-7@1	-25.7	0.04	-12.9	2.83	46.7	0.17	Dark
E180-7@2	-26.3	0.03	N.A.	N.A.	N.A.	N.A.	Dark
E180-9@1	-23.8	0.03	-6.5	1.33	286.4	0.24	Bright
E180-10@1	-25.4	0.04	20.8	2.11	87.4	0.15	Intermediate
E180-10@2	-24.7	0.04	25.5	1.91	120.5	1.64	Bright
E183-3@1	-24.7	0.04	N.A.	N.A.	N.A.	N.A.	Bright
E183-3@2	-24.9	0.05	N.A.	N.A.	N.A.	N.A.	Bright
E183-4@1	-24.3	0.05	N.A.	N.A.	N.A.	N.A.	Dark
E183-9@1	-25.7	0.05	N.A.	N.A.	N.A.	N.A.	Bright
E184-2@1	-26.5	0.03	-10.5	4.57	37	0.1	Dark
E184-2@2	-26	0.04	N.A.	N.A.	N.A.	N.A.	Dark
E184-3@1	-26.2	0.04	13.2	1.72	172	0.38	Bright
E184-4@1	-25.7	0.05	-10.1	3.15	46.9	0.18	Dark
E184-9@1	-27.4	0.04	-4.5	2.1	156.6	2.19	Bright
E184-9@2	-27.6	0.04	3.2	1.69	160.8	0.35	Bright
MIN	-27.6		-12.9		37		
MAX	-23.8		25.5		286.4		
AVG	-25.8		1.9		135		

Note: N.A. = not analysis

Always consult and cite the final, published document. See http:/www.minsocam.org or GeoscienceWorld

Table 2. Observed lattice parameters of perovskite of inclusion no. 3.

d_{hkl} observed	Ca-silicate perovskite orthorhombic Li et al. (2006)	Ca-silicate perovskite tetragonal Caracas and Wentzcovitch (2006)
	a_0 = 1.0000 nm b_0 = 1.0059 nm c_0 = 0.7018 nm	a_0 = 0.49812 nm b_0 = 0.49812 nm c_0 = 0.7182 nm
0.298 nm	0.30256 nm (0-3-1)/(031)	0.31624 nm (11-1)/(-1-11)
0.279 nm	0.28845 nm (3-11)	0.29130 nm (012)
0.216 nm	0.21783 nm (322)	0.21277 nm (121)
0.193 nm	0.20076 nm (-3-40)	0.21577 nm (-103)
angles between adjacent planes		
49.7°	48.82° (322)/(031)	46.91° (121)/(11-1)
47°	45.85° (322)/(3-11)	42.28° (121)/(012)
41°	41.40° (-3-40)/(3-11)	43.02° (-103)/(012)
43°	43.92° (-3-40)/(0-3-1)	47.79° (-1-11)/(-103)

Always consult and cite the final, published document. See http:/www.minsocam.org or GeoscienceWorld

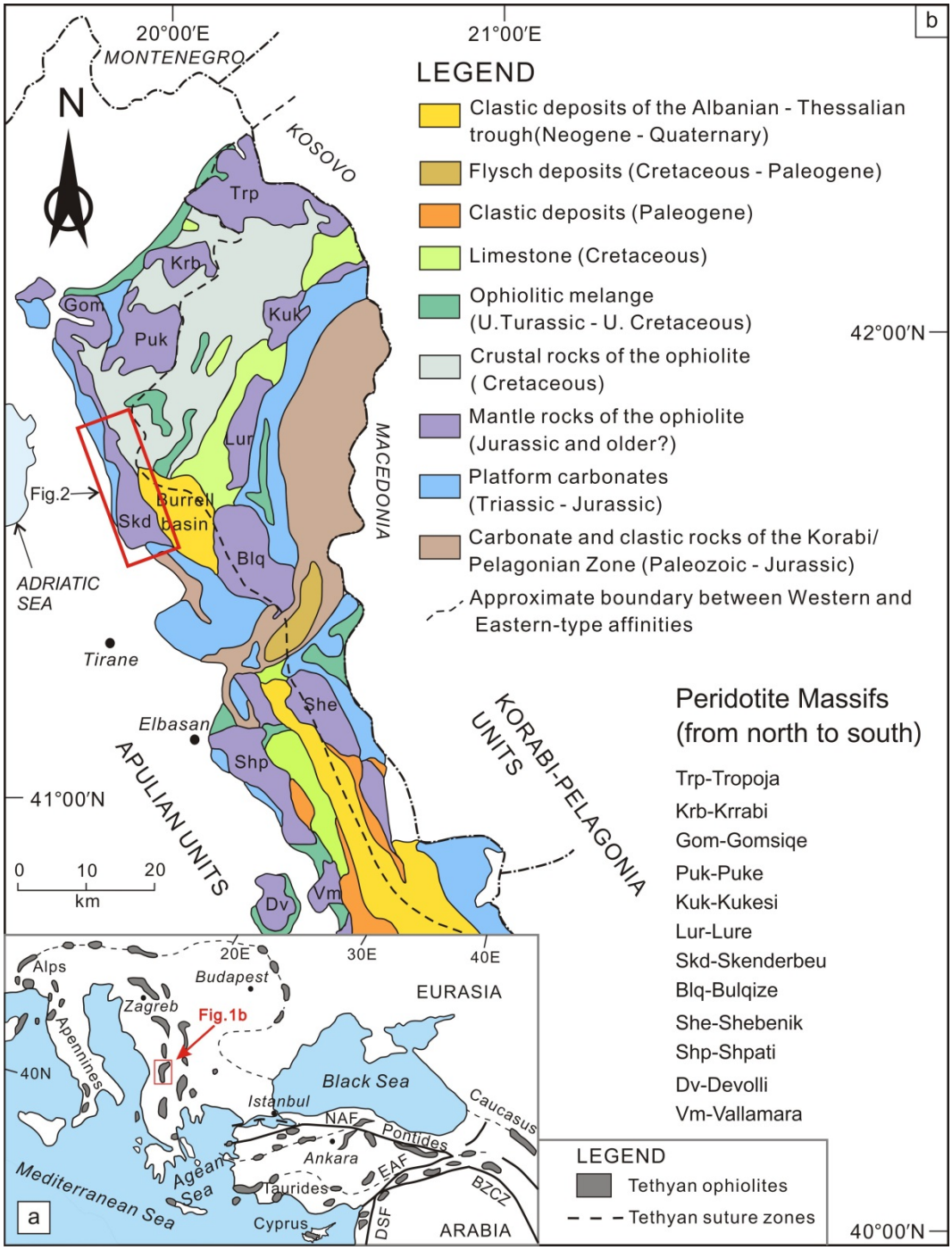

Fig. 1

Always consult and cite the final, published document. See http:/www.minsocam.org or GeoscienceWorld

This is a preprint, the final version is subject to change, of the American Mineralogist (MSA)
Cite as Authors (Year) Title. American Mineralogist, in press.
DOI: https://doi.org/10.2138/am-2019-6751

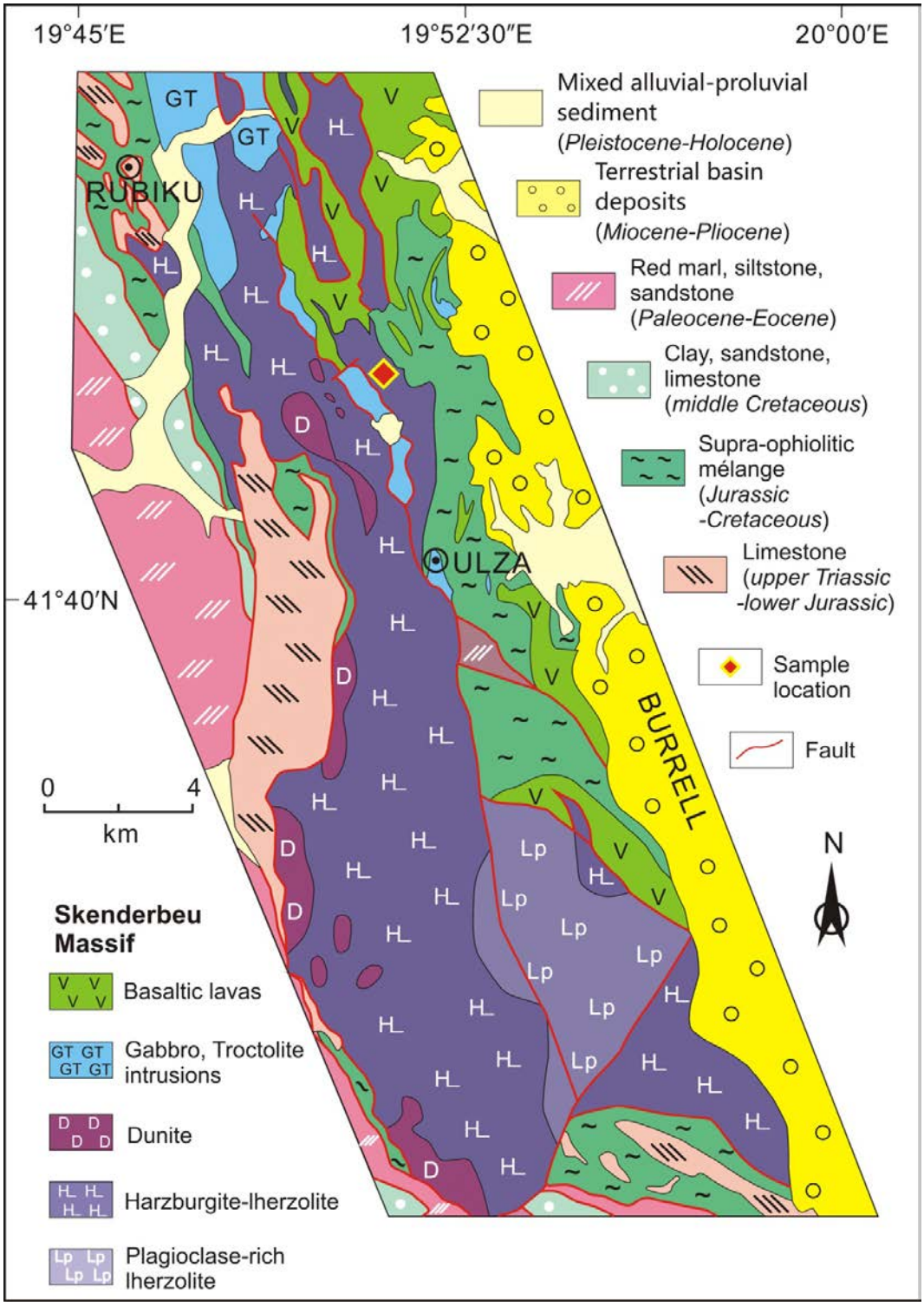

Fig. 2

Always consult and cite the final, published document. See http:/www.minsocam.org or GeoscienceWorld

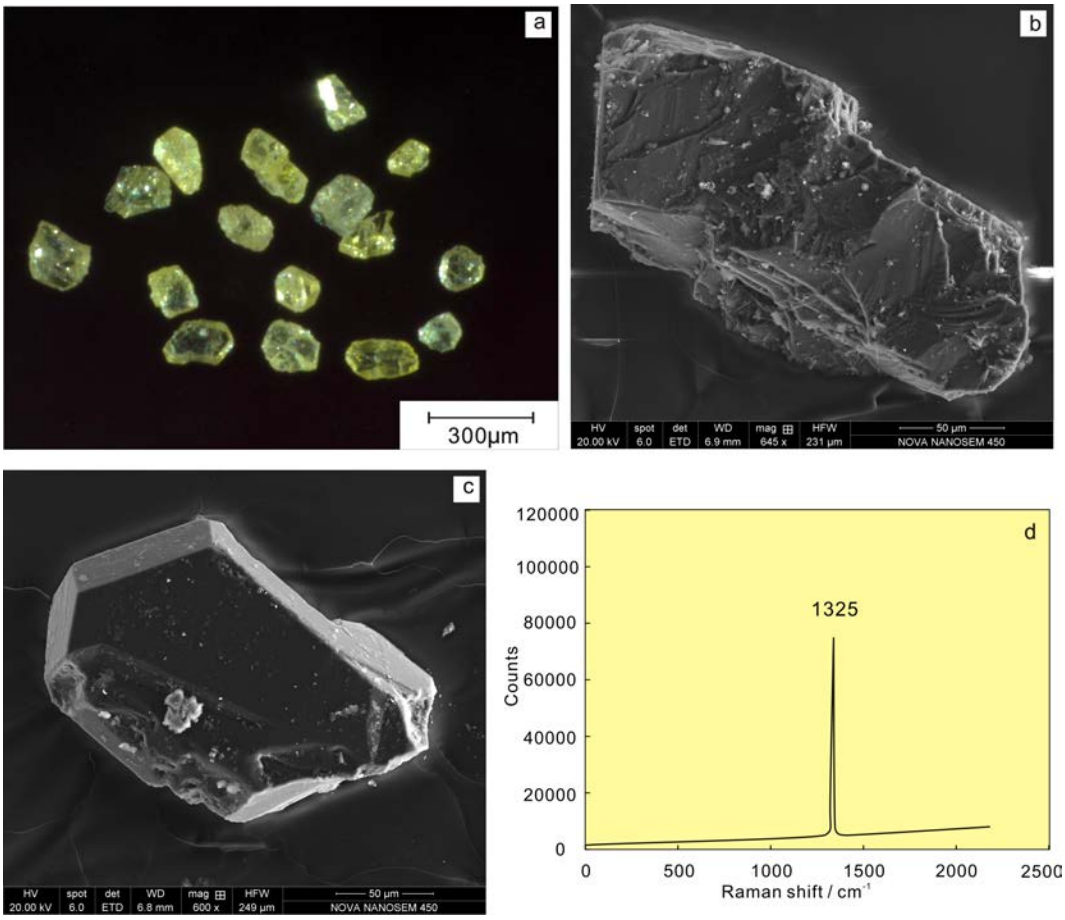

Fig. 3

Always consult and cite the final, published document. See http:/www.minsocam.org or GeoscienceWorld

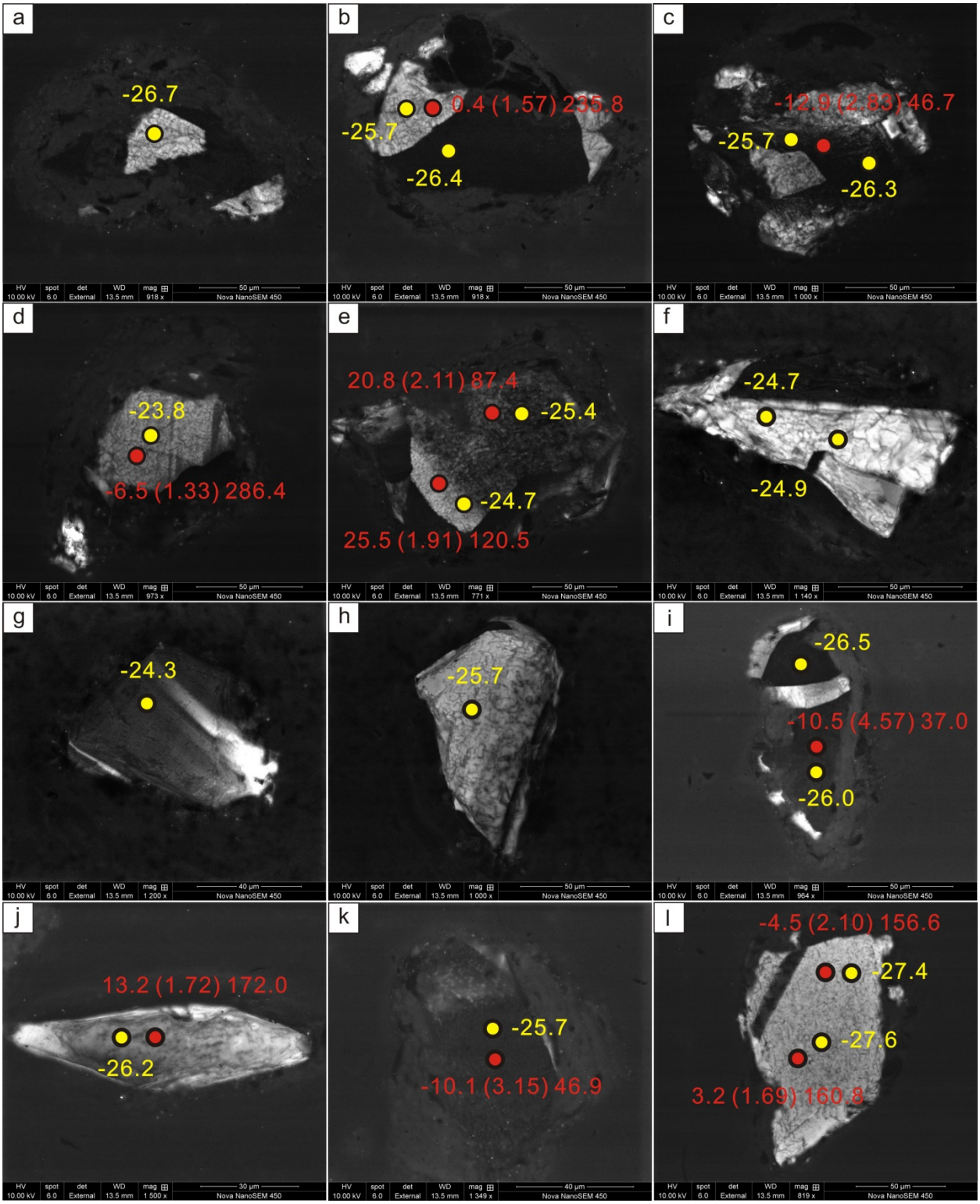

Fig. 4

Always consult and cite the final, published document. See http:/www.minsocam.org or GeoscienceWorld

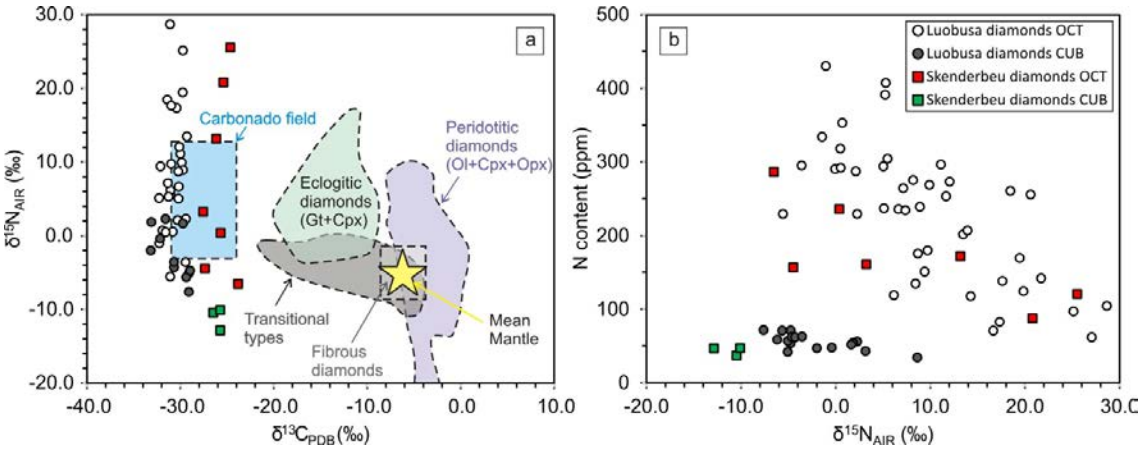

Fig. 5

Always consult and cite the final, published document. See http:/www.minsocam.org or GeoscienceWorld

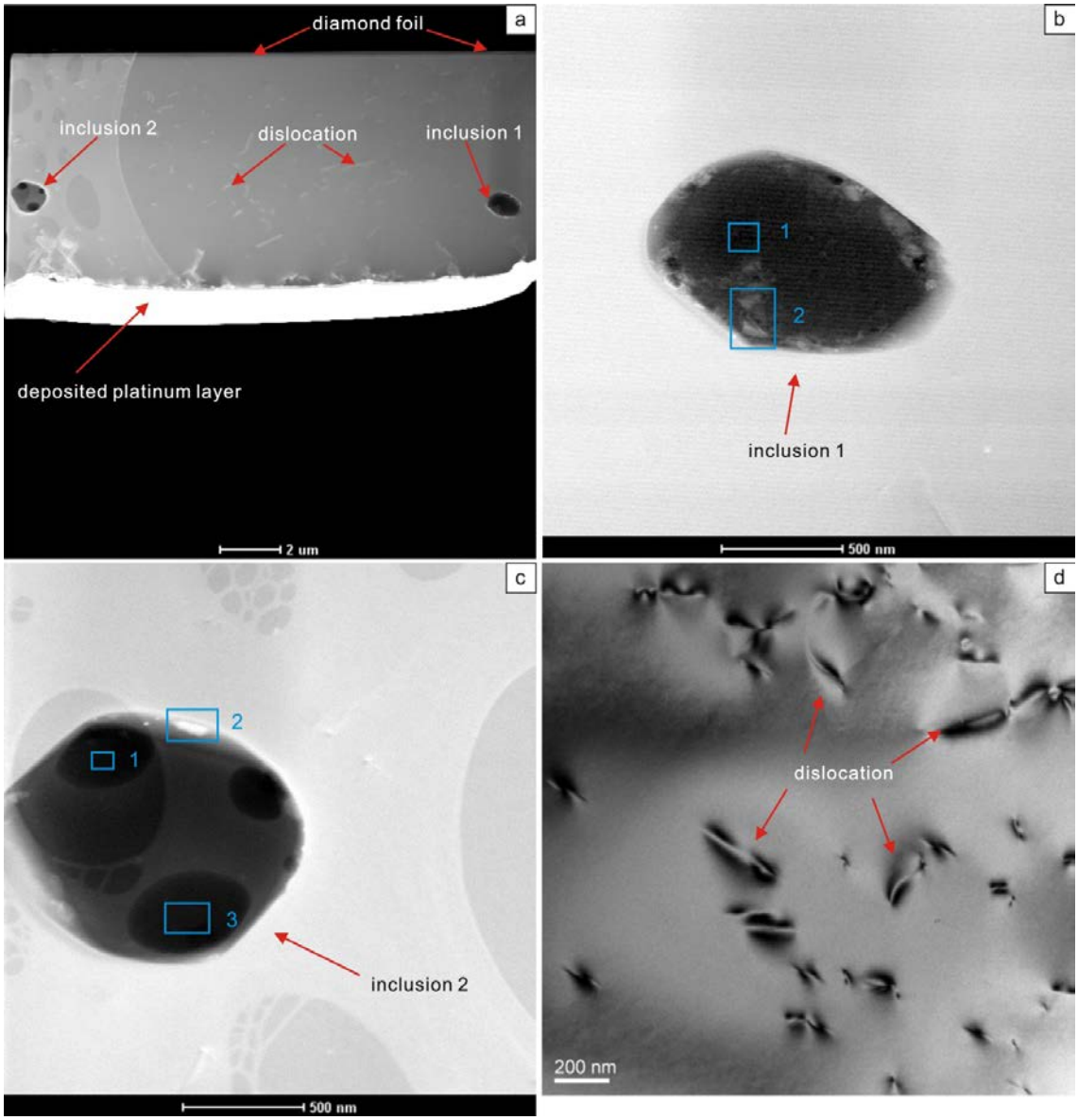

Fig. 6

Always consult and cite the final, published document. See http:/www.minsocam.org or GeoscienceWorld

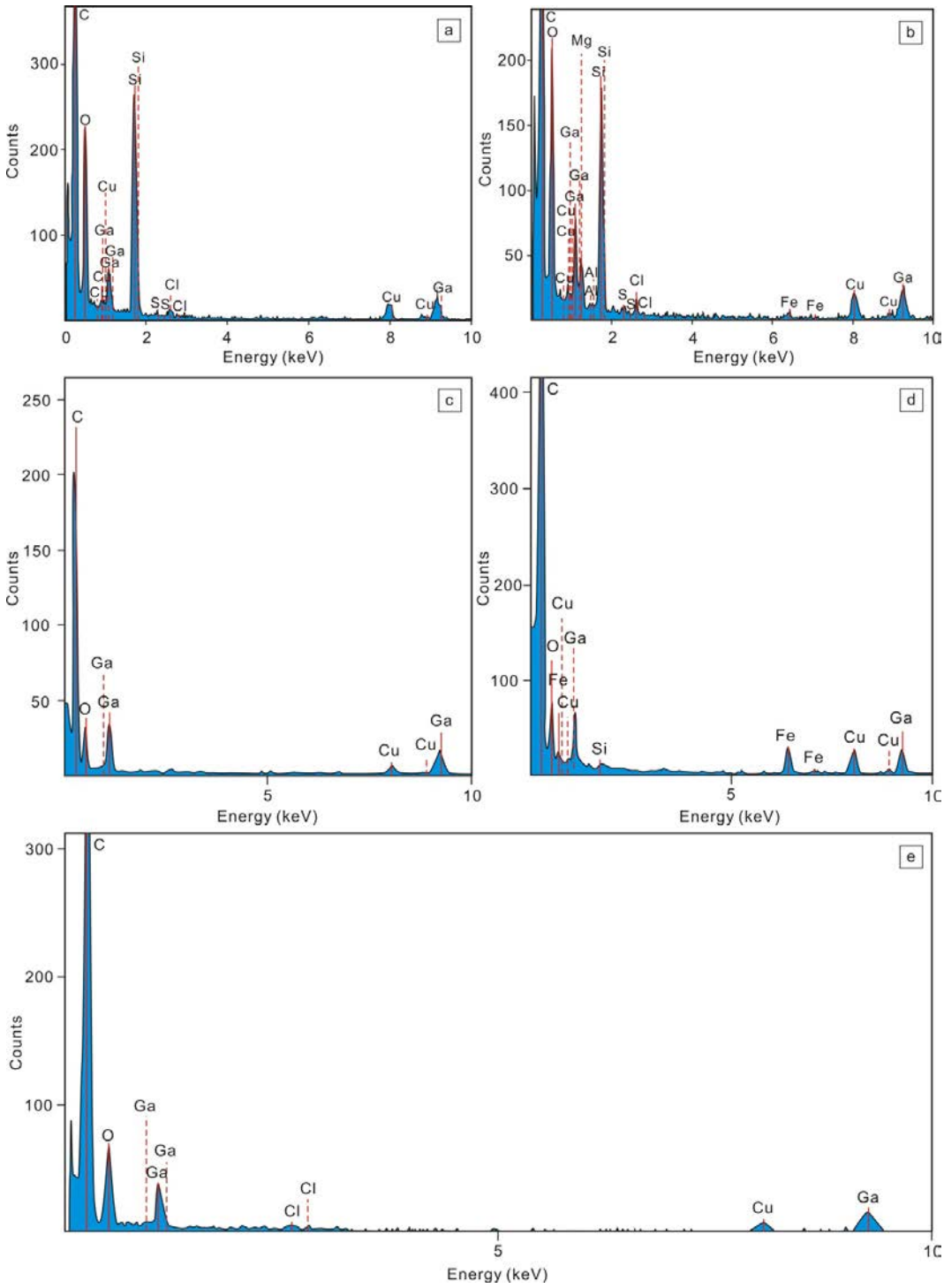

Fig. 7

Always consult and cite the final, published document. See http:/www.minsocam.org or GeoscienceWorld

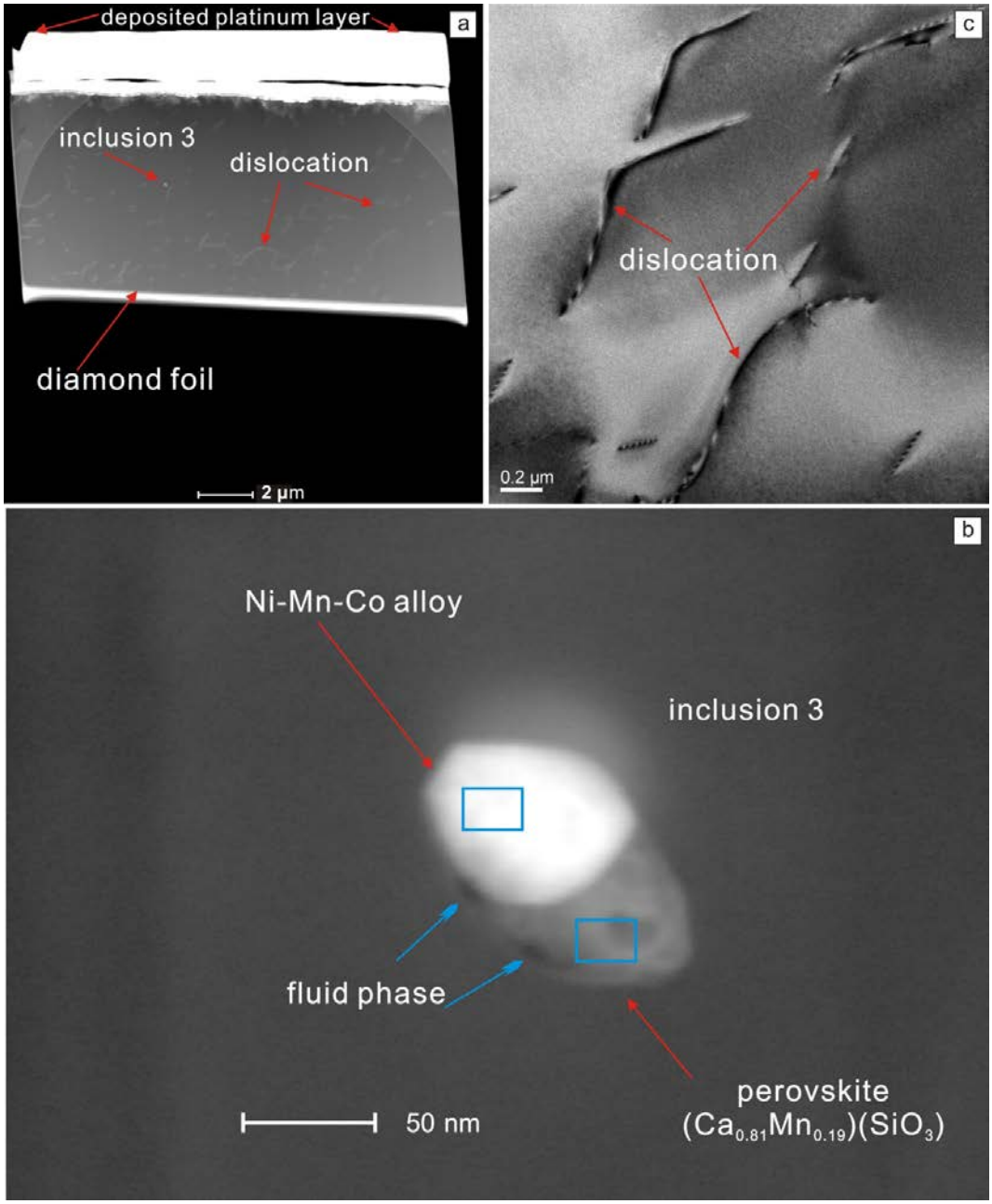

Fig. 8

Always consult and cite the final, published document. See http:/www.minsocam.org or GeoscienceWorld

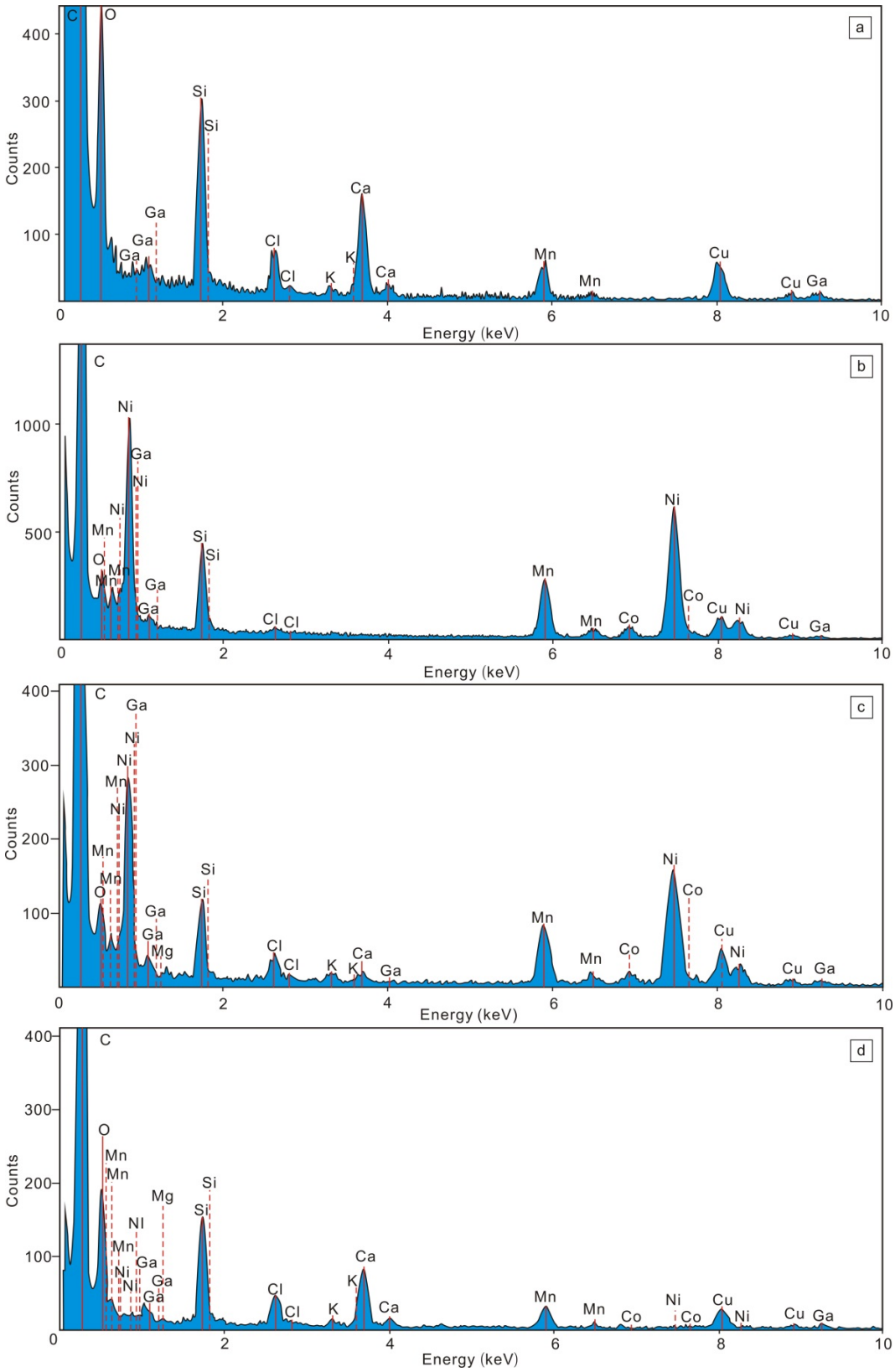

Fig. 9

Always consult and cite the final, published document. See http:/www.minsocam.org or GeoscienceWorld

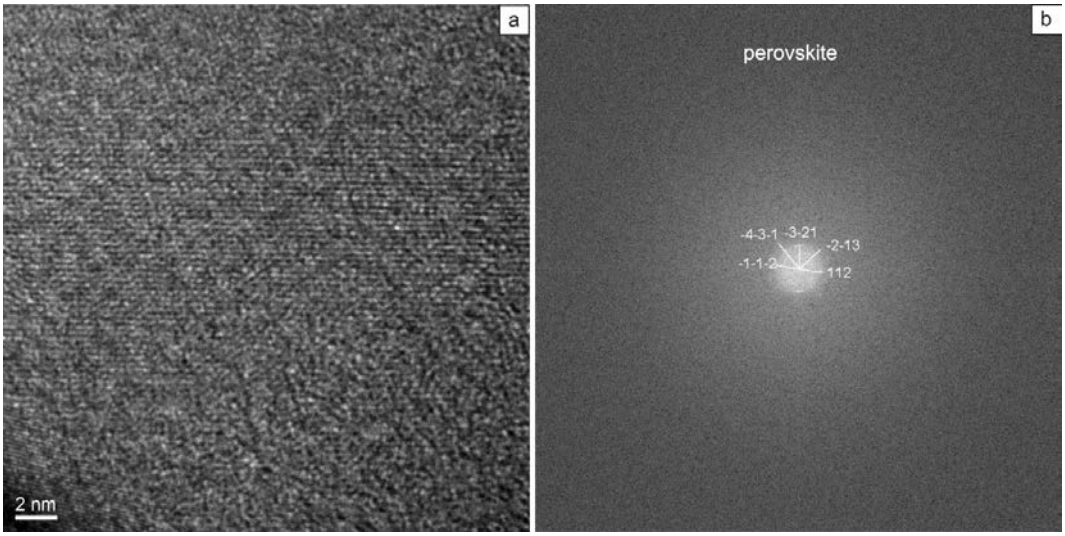

Fig. 10

Always consult and cite the final, published document. See http:/www.minsocam.org or GeoscienceWorld

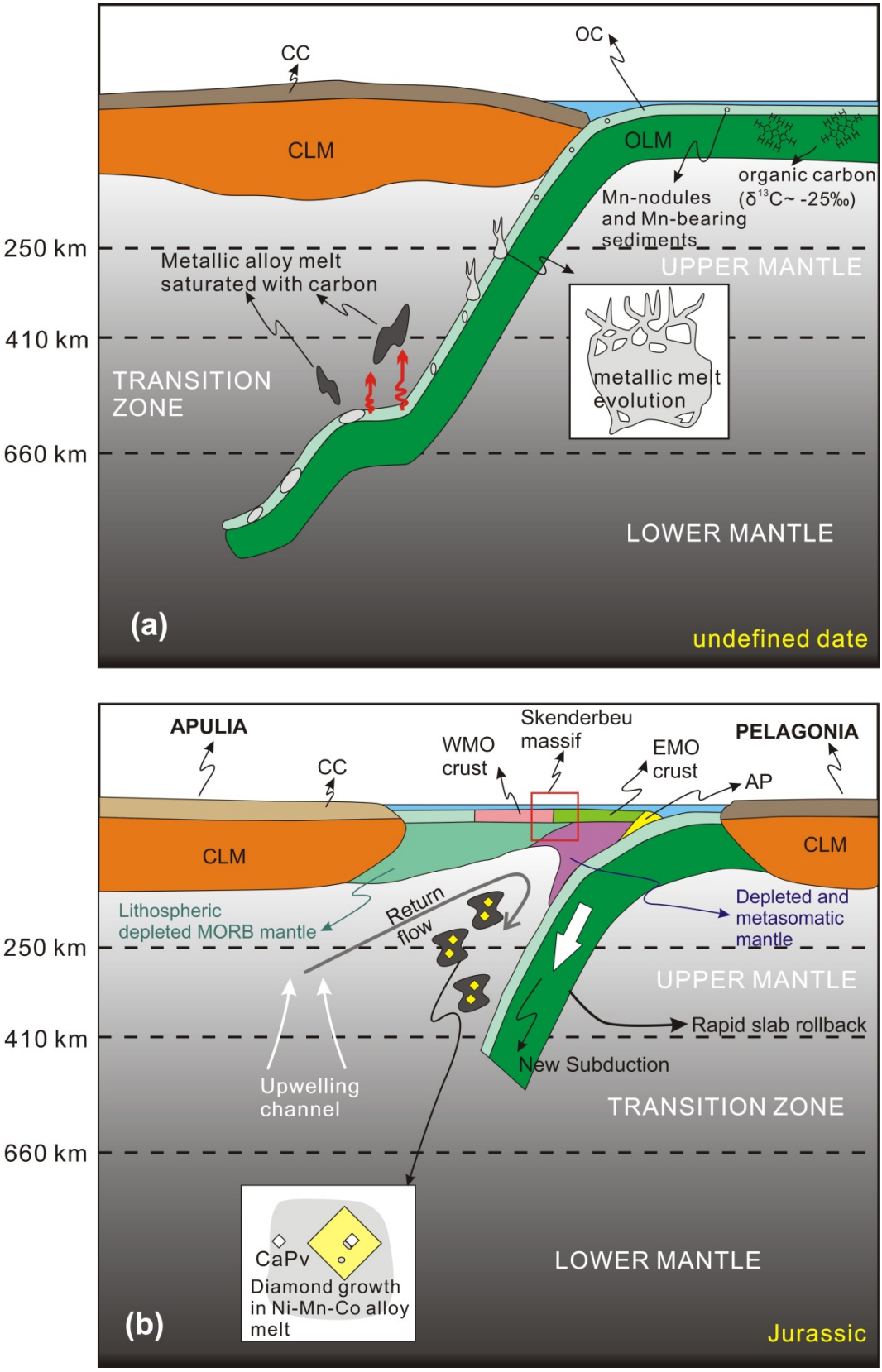

Fig. 11

Always consult and cite the final, published document. See http:/www.minsocam.org or GeoscienceWorld